From the Klinik für Radiologie und Neuroradiologie
(Director: Prof. Dr. med. Olav Jansen)
at the University Medical Centre Schleswig-Holstein, Campus Kiel
at Christian-Albrechts-Universität zu Kiel - Kiel University

# Detection of cervical and thoracic multiple sclerosis lesions of the spinal cord using a 3D phase-sensitive inversion recovery (PSIR) magnetic resonance imaging technique at 1.5T

Dissertation
to acquire the doctoral degree (Dr. med.)
at the Faculty of Medicine
at Christian-Albrechts-Universität zu Kiel - Kiel University

presented by
Fernando Bueno Neves
from Florianópolis

Kiel 2026

1st Reviewer: PD Dr. habil. Dipl.-Phys. Mona Salehi Ravesh

2nd Reviewer: Prof. Dr. med. Frank Leypoldt

Date of oral examination: 06.07.2026

Approved for printing, Kiel, 20.03.2026

Signed: Prof. Dr. Franziska Theilig

(Chairperson of the Examination Committee)

For all the people who struggle with multiple sclerosis. Here’s to hoping I can shed a small light on the dark corners of this disease.

# Table of Contents

Table of Contents ..... I

Tables and Figures ..... III

List of Abbreviations ..... IV

1 Introduction ..... 1

1.1 A brief history of multiple sclerosis ..... 1

1.2 Multiple sclerosis: the current state of knowledge ..... 2

1.2.1 Prevalence and Incidence ..... 2

1.2.2 Environmental Factors ..... 2

1.2.3 Gender differences ..... 4

1.2.4 Age of Onset and Progression ..... 4

1.2.5 The Expanded Disability Status Scale ..... 5

1.3 MRI of the spinal cord and its challenges ..... 6

1.4 Imaging in multiple sclerosis ..... 7

1.4.1 Cross-sectional imaging and the McDonald criteria ..... 7

1.4.2 Current MRI practice in cerebral and spinal MS ..... 10

1.4.3 The role of contrast-enhanced T1-weighted pulse sequences ..... 11

1.5 Hypothesis ..... 13

2 Methods ..... 14

2.1 Ethical considerations ..... 14

2.2 Study population ..... 14

2.3 MRI equipment and imaging pulse sequences ..... 14

2.4 Image analysis and quality assessment ..... 15

2.5 Analysis of contrast-enhanced 2D T1-weighted TSE sequences ..... 20

2.6 Statistical analysis ..... 20

3 Results ..... 22

3.1 Population ..... 22

3.2 Lesion count and distribution ..... 23
3.3 Imaging Quality Assessment ..... 26
3.4 Lesion detection rates ..... 26
3.5 Lesion-to-cord contrast ratio (CR) analysis ..... 27
3.6 Certainty of lesion count ..... 28
3.7 Contrast-enhanced 2D T1-weighted TSE sequences ..... 28
4 Discussion ..... 29
4.1 Population ..... 29
4.1.1 Drug regimens ..... 30
4.2 Diagnosis and disease monitoring through the 3D T1-weighted PSIR technique ..... 31
4.2.1 Inter-rater variability ..... 32
4.2.2 Lesion detection and interpretation ..... 33
4.2.3 Clinical applicability ..... 35
4.3 The use of gadolinium in spinal studies of patients with confirmed MS ..... 35
4.4 Limitations ..... 36
5 Summary ..... 38
6 References ..... 39
Appendix ..... 45
Appendix 1: Approved Ethical Committee Application ..... 45
Thanks & Acknowledgments ..... 46
Publications ..... 47

## Tables and Figures

Table 1: The Expanded Disability Status Scale (EDSS).

Table 2: Evidence needed to secure an MS diagnosis and the McDonald criteria.

Table 3: Pulse sequence parameters.

Table 4: Population data.

Table 5: Lesion count according to pulse sequence and rater.

Table 6: Analysis of the imaging quality of the different sequences is demonstrated for the cervical spinal cord, the thoracic spinal cord, and the medullary cone.

Table 7. Lesion-to-cord contrast ratio values for each imaging dataset and spinal segment.

Table 8: Certainty of lesion count.

Figure 1: A periventricular white matter lesion in a patient with known multiple sclerosis as seen on MRI (left) and CT (right).

Figure 2: Comparison of a juxtacortical lesion on FLAIR and DIR.

Figure 3: Cervical lesions observed on sagittal $T_2$-weighted TSE, sagittal $T_2$-weighted STIR, and 3D $T_1$-weighted PSIR.

Figure 4: Overview of imaging quality.

Figure 5: Axial $T_2$-weighted TSE and $T_1$-weighted PSIR images of a lateral cervical lesion.

Figure 6: ROI measurements of the same cervical lesion in the sagittal plane on $T_2$-weighted STIR and $T_2$-weighted TSE.

Figure 7: Current therapy regimens in the study population.

Figure 8: Anatomical distribution of lesions (sagittal plane).

Figure 9: Anatomical distribution of lesions (axial plane).

Figure 10: Lesion detection rates in the consensus reading.

Figure 11: Comparison of a cervical lesion on 2D $T_2$-weighted TSE and postcontrast 2D $T_1$-weighted TSE.

Figure 12. Blurry versus well-defined lesions on 2D $T_2$-weighted PSIR.

## List of Abbreviations

| | |
|---|---|
| BMI | Body mass index |
| CE | contrast enhanced |
| CIS | clinically isolated syndrome |
| CNS | Central nervous system |
| CR | Contrast Ratio |
| DIR | Double Inversion Recovery |
| DIS | Dissemination in space |
| DIT | Dissemination in time |
| EAE | Experimental autoimmune encephalomyelitis |
| EBV | Epstein-Barr virus |
| EDSS | Expanded Disability Status Scale |
| FA | flip angle (degree) |
| FOV | field of view (in mm) |
| FS | Functional system |
| GBCA | gadolinium-based contrast agent |
| ICC | interclass correlation coefficient |
| MRI | Magnetic resonance imaging |
| MS | Multiple sclerosis |
| PPMS | Primary progressive multiple sclerosis |
| PSIR | Phase-Sensitive Inversion-Recovery |
| RRMS | Relapsing-remitting multiple sclerosis |
| SL | slice thickness (in mm) |
| SPMS | Secondary progressive multiple sclerosis |
| STIR | Short tau inversion recovery |
| TE | time of echo (in ms) |
| TR | time of repetition (in ms) |
| TSE | turbo spin echo |
| WHO | World Health Organization |

# 1 Introduction

Multiple sclerosis (MS) is a neurological disorder known for its debilitating progression and clinical complexity. It is characterized by chronic inflammation, primarily caused by lymphocytic infiltration, resulting in demyelination and axonal damage [1]. In modern medical practice, the diagnosis and management of MS are closely linked with medical imaging, with magnetic resonance imaging (MRI) playing a central role.

## 1.1 A brief history of multiple sclerosis

Even though MS keeps eluding clinicians to this day, its first documented anecdotes trace back to the mid-19th century, notably the case of Sir Augustus D'Este. His diary, one of the earliest known records of MS, portrays the condition [2,3]. Written in the mid-1800s, D'Este's entries describe a progression of symptoms now considered classic indicators of the disease. His initial experiences, believed to be retrobulbar neuritis, began at a relatively young age. Over time, the symptoms D'Este recorded — including severe numbness, spasms, mood disorders, and gait abnormalities — resemble our present-day understanding of the clinical presentation of MS [2,3].

These journal entries, however, are mostly anecdotal and do not characterize the disease formally. The first scientific acknowledgment of MS dates to the nineteenth century, through the French neurologist Jean-Martin Charcot [2-4]. Not only did he dissect the various presentations of the disease, delineating its cerebral, spinal, and mixed cerebrospinal forms, but he also recognized microscopic sclerotic plaques — hardened patches that would give multiple sclerosis its name [3,4].

Further advancements added to the understanding of MS as an immune-mediated condition. This progress was particularly influenced by the development of experimental autoimmune encephalomyelitis (EAE), an animal model that should mirror the characteristics of multiple sclerosis. It has been described that central nervous system lesions with a predilection for the white matter, perivascular position, and demyelination could be experimentally induced in monkeys [5]. In a 1946 study, Kabat et al. [5] injected emulsions composed of different tissues from monkeys and rabbits into thirty rhesus monkeys and found that the exposure to heterologous and homologous brain tissue induced ataxia, paresis, and visual abnormalities in some test subjects. The authors noted that such symptoms resembled acute disseminated encephalomyelitis in humans, potentially helping to elucidate the mechanism of demyelinating diseases.

During the latter half of the 20th century, there was a significant evolution in understanding the pathological mechanisms of MS and its treatment. Acknowledging the immune system's central role in the disease's pathogenesis led to the development of immunomodulatory therapies. The 1990s marked a critical period with the introduction of disease-modifying therapies for MS, such as interferon-beta [6]. In a 1996 publication, through a randomized, double-blinded, placebo-controlled trial phase of interferon beta-Ia, Jacbos et al. [6] observed that patients who received the medication had delayed symptomatic progression and presented fewer exacerbations.

## 1.2 Multiple sclerosis: the current state of knowledge

### 1.2.1 Prevalence and Incidence

The global distribution of MS has garnered significant interest among researchers and healthcare professionals. This chronic, immune-mediated neurological disorder is found worldwide, but its prevalence and impact vary across different regions.

The "Atlas of Multiple Sclerosis," in its latest 2020 edition, presents a comprehensive analysis of the disease's epidemiology [7]. This edition reports an increase in global MS prevalence to approximately 36 cases per 100,000 people, exceeding previous estimates. The atlas attributes this rise to factors such as enhanced diagnostic methods and greater accessibility to healthcare [7,8], along with an increase in the life expectancy of MS patients [7,9]. This data underscores a growing incidence of MS in all the regions recognized by the World Health Organization (WHO) since the previous 2013 report.

Specific continents and countries have been identified as hotspots for MS, with Europe and North America having the highest prevalence rates. According to the latest edition of the "Atlas of Multiple Sclerosis" [7], MS prevalence is reported as 143 per 100,000 in Europe and 118 per 100,000 in the Americas. These figures exceed the global average of 44 per 100,000 and are much higher compared to regions like Southeast Asia, where the prevalence is as low as 9 per 100,000 [7].

The reasons behind such stark regional differences in MS prevalence are a subject of ongoing debate and research. It's speculated that both environmental factors and gender differences play a role.

### 1.2.2 Environmental Factors

A prominent research focus is the association between vitamin D deficiency — often caused by limited sunlight exposure — and MS. This relationship is complex and multifaceted, as outlined in “Vitamin D and multiple sclerosis: An update” [10]. This study explores how reduced sun exposure, leading to vitamin D insufficiency, is prevalent in temperate areas and correlates with a higher MS risk. Moreover, the role of vitamin D in MS extends to immunomodulation and potentially influences the immune and central nervous systems. The update conducted by Zahoor and Haq also discusses the potential role of vitamin D supplementation as a cost-effective therapy for MS, even if major concerns about its safety, dosage, and response exist [10].

In addition to the vitamin D hypothesis, other environmental factors are key to understanding MS. One such factor is the Epstein-Barr virus (EBV). This common herpes virus has been consistently linked to MS [11]. Over 90% of the global population comes across EBV during their lifetime [7], and research by Kjetil Bjornevik et al. indicates that previous EBV infection may raise the risk of developing MS [11].

The prevalence of MS exhibits a notable latitude gradient, with increasing cases as one moves further from the equator. This pattern has been associated with variations in sunlight exposure, which, in turn, affects vitamin D levels. Regions with higher latitudes receive less sunlight, particularly during winter, resulting in vitamin D deficiency. A comprehensive meta-analysis has confirmed a significant positive association between MS prevalence and latitude, suggesting environmental factors such as ultraviolet radiation and vitamin D as key contributors [12]. Furthermore, a study examining the roles of melatonin and vitamin D in MS indicates that vitamin D decreases while melatonin increases beyond 37° latitude, impacting the prevalence of the disease [13].

Smoking is another environmental factor that has received considerable attention. A range of epidemiological studies have indicated that smoking not only elevates the risk of developing MS but may also worsen the disease’s progression in those already diagnosed [14-17]. In his 2012 review, Wingerchuk highlights evidence that suggests a greater risk of conversion from relapsing-remitting (RRMS) to secondary progressive MS and from clinically isolated syndrome (CIS) to confirmed MS in smokers [14]. Additionally, there is evidence linking psychological and psychiatric conditions such as depression to the prevalence of MS [17].

Recent research has highlighted the potential link between obesity during adolescence and the risk of developing MS later in life. A study by Harroud et al. [18] found that higher body mass index (BMI) in childhood was associated with an increased likelihood of MS, suggesting a possible causal relationship. The study indicates that persistent obesity from childhood into early adulthood might mediate this association, independent of pubertal timing.

These findings further reinforce the hypothesis that environmental influences may play a relevant role in the onset and progression of MS, as vitamin D levels, infections, sun exposure, smoking, obesity, and even psychological factors have been thoroughly examined.

### 1.2.3 Gender differences

Some authors have examined the potential influence of female hormones in the development of MS, especially estrogen. Estrogen, recognized for its immunomodulatory effects, fluctuates during the reproductive years in women and sinks after menopause. These hormonal changes are thought to impact autoimmune responses, potentially explaining the observed variations in MS severity and onset among women. Besides the disease being more prevalent in women, it is also associated with an earlier onset, with more frequent relapses. However, it is linked to worse outcomes in males [19]. Yasrraelit and Correale [19] support that the gender differences in the presentation and course of MS might also be attributable to puberty, pregnancy, puerperium, and menopause.

Yasrraelit and Correale also summarize the estrogen-induced immunomodulatory effects in MS patients by discussing a possible paradox. While estrogen promotes anti-inflammatory effects in EAE, it is observed to be associated with pro-inflammatory changes in chronic autoimmune diseases [19].

### 1.2.4 Age of Onset and Progression

Multiple sclerosis predominantly impacts individuals between 20 and 50 years of age [7].

In terms of presentation and progression, MS exhibits significant variations. Over the decades, different classifications have been established. Currently, some patterns have been used to describe longitudinal disease: relapsing-remitting (RRMS), secondary progressive (SPMS), primary progressive (PPMS), and benign [20,21]. As with other classifications employed since the nineteenth century, these patterns overlap.

RRMS is described as the most common presentation, with patients exhibiting phases of recovery between relapses. SPMS is associated with disease progression between the periodic symptoms, with clinical deficits becoming permanent and progressively more recognizable. PPMS represents less frequent cases (around 10%) associated with an accumulation of disability for over a year after onset, with no typical remission. Lastly, benign multiple sclerosis, a fundamentally retrospective diagnosis, represents the cases associated with preserved patient functionality for over 15 years [20, 21].

Some authors argue against classifying MS into separate clinical entities, though. Instead, they regard it as a spectrum that should not be artificially divided into discrete and arbitrary boundaries. Dobson and Giovannoni [4] support this perspective. These researchers contend that the categorization of MS into distinct diseases was primarily influenced by the efforts of the pharmaceutical industry to get interferon beta licensed under the Orphan Drug Act in the USA. They describe MS as a continuum of pathological changes that do not correspond to distinct clinical entities and argue that this understanding aligns with the gradual clinical progression from RRMS to SPMS.

Dobson and Giovannoni [4] also detail the course of MS as a "journey from being at risk, through asymptomatic, prodromal, and symptomatic phases of the disease." They concur with contemporary research, noting that MS is typically suspected following presentations of clinically isolated syndrome (CIS) [4].

### 1.2.5 The Expanded Disability Status Scale

Various scores and classification systems have been developed to diagnose and manage MS. Among these, the Expanded Disability Status Scale (EDSS) is a commonly used tool for assessing the level of disability in MS patients [22].

The EDSS is a tool intended for the clinical assessment of disease progression. Introduced by John Kurtzke in the early 1980s [22], this scale provides a standardized measurement of physical disability in MS patients, with scores ranging from 0 (normal neurological examination) to 10 (death due to MS). The granular nature of the EDSS allows for the objective quantification of neurological impairment, assisting clinicians in tracking disease trajectory, making therapeutic decisions, and facilitating comparisons across different clinical studies. As such, it was established as a parameter for the primary outcome in interferon beta I-a trials [5]. Since then, it has been widely adopted in clinical trials and real-world settings, providing invaluable data for evaluating therapeutic interventions and helping shape treatment paradigms [23].

Despite its widespread use, it is imperative to understand the EDSS's limitations. One of the main criticisms concerns the disproportionate emphasis on ambulation over other neurological functions, which can sometimes overlook significant disability [24].

THE EDSS is presented in its entirety in Table 1.

| | |
|---|---|
| 0 | Normal neurological exam, no disability in any functional system (FS) |
| 1.0 | No disability, minimal signs in one FS |
| 1.5 | No disability, minimal signs in more than one FS |
| 2.0 | Minimal disability in one FS |
| 2.5 | Mild disability in one FS or minimal disability in two FS |
| 3.0 | Moderate disability in one FS, or mild disability in three or four FS. No impairment to walking |
| 3.5 | Moderate disability in one FS and more than minimal disability in several others. No impairment to walking |
| 4.0 | Significant disability but self-sufficient and up and about some 12 hours a day. Able to walk without aid or rest for 500m |
| 4.5 | Significant disability but up and about much of the day, able to work a full day, may otherwise have some limitation of full activity or require minimal assistance. Able to walk without aid or rest for 300m |
| 5.0 | Disability severe enough to impair full daily activities and ability to work a full day without special provisions. Able to walk without aid or rest for 200m |
| 5.5 | Disability severe enough to preclude full daily activities. Able to walk without aid or rest for 100m |
| 6.0 | Requires a walking aid – cane, crutch, etc. – to walk about 100m with or without resting |
| 6.5 | Requires two walking aids – pair of canes, crutches, etc. – to walk about 20m without resting |
| 7.0 | Unable to walk beyond approximately 5m even with aid. Essentially restricted to wheelchair; though wheels self in standard wheelchair and transfers alone. Up and about in wheelchair some 12 hours a day |
| 7.5 | Unable to take more than a few steps. Restricted to wheelchair and may need aid in transfering. Can wheel self but cannot carry on in standard wheelchair for a full day and may require a motorised wheelchair |
| 8.0 | Essentially restricted to bed or chair or pushed in wheelchair. May be out of bed itself much of the day. Retains many self-care functions. Generally has effective use of arms |
| 8.5 | Essentially restricted to bed much of day. Has some effective use of arms retains some self-care functions |
| 9.0 | Confined to bed. Can still communicate and eat |
| 9.5 | Confined to bed and totally dependent. Unable to communicate effectively or eat/swallow |
| 10.0 | Death due to MS |

Table 1: The Expanded Disability Status Scale (EDSS).

### 1.3 MRI of the spinal cord and its challenges

The first MRI publications in Acta Radiologica — a peer-reviewed radiology journal established in 1921 and initially published only in German — appeared in 1984, four years

after the commercial release of the first MRI systems [25]. In its first two years, all MRI-related research articles came from the United States [25]. Nowadays, however, MRI-related papers comprise 30% to 40% of the journal's original articles, having reached 49% in 2019 [25]. This illustrates the rapid evolution of MRI's role in radiology practice and research.

Since the early stages of MRI, spinal cord imaging has been challenging due to its proximity to the vertebral column, small size, and motion from patient breathing and cerebrospinal fluid pulsation. The 1980s and 1990s, however, saw significant advancements with the advent of optimized sequences, such as short-tau inversion recovery (STIR). These sequences use fat suppression to possibly improve the detection of spinal cord lesions when compared to fast spin-echo pulse sequences, usually having longer acquisition times as a tradeoff [26].

Anatomically, the spinal cord stretches from the corticomedullary junction at the foramen magnum of the skull down to the medullary cone, spanning a length of approximately 42 to 45 cm while maintaining a diameter of around 1 cm [4]. Its slender, elongated tubular structure makes the spinal cord susceptible to motion artifacts, especially in the thoracic region.

Motion artifacts remain one of the biggest challenges in spinal cord imaging. Unlike the relatively stable brain, the spinal cord is more susceptible to movement, influenced by patient breathing, heartbeat, and involuntary muscle contractions. Even minor movements can lead to blurred images or ghosting artifacts. Additionally, at a higher field strength of 3T, motion artifacts and magnetic field inhomogeneities are more pronounced than at 1.5T [27]. This issue is particularly noticeable in sequences with longer acquisition times, like STIR and PSIR [26].

## 1.4 Imaging in multiple sclerosis

### 1.4.1 Cross-sectional imaging and the McDonald criteria

Cross-sectional imaging has been established as the method of choice for diagnosing and monitoring multiple sclerosis.

Computed tomography (CT) imaging plays a limited role, though, as it often reveals non-specific findings. Detectable abnormalities involve brain atrophy, areas of hypoattenuation in the white matter and periventricular spaces, and areas of abnormal enhancement [28]. The following image compares the same periventricular lesion in a patient evaluated on MRI and CT:

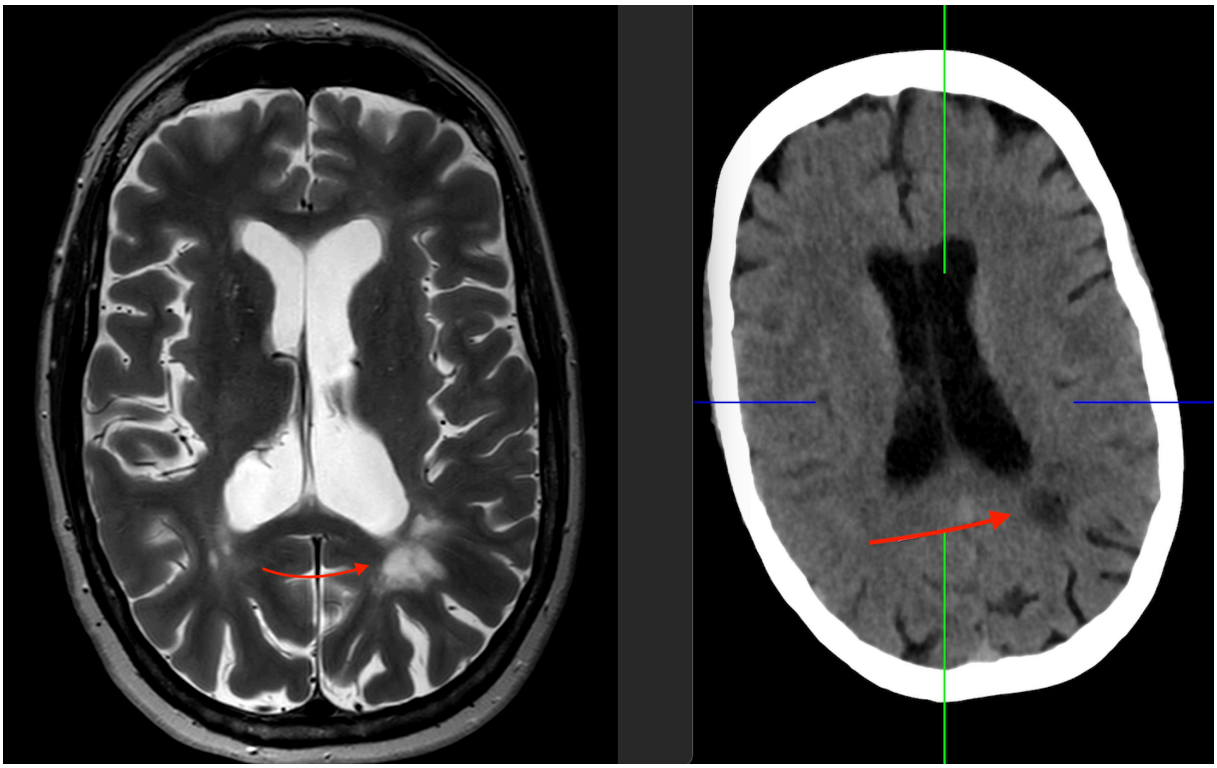

Figure 1: A periventricular white matter lesion in a patient with known multiple sclerosis as seen on MRI (left) and CT (right). On MRI (left), the periventricular white matter lesion presents itself as an irregular, blurred hyperintense lesion in an 2D axial $T_2$-weighted sequence. It correlates with a blurred hypodense lesion on CT (right).

Loizou et al. attempted to categorize the CT changes in the brain affected by multiple sclerosis in the early 1980s. They concluded that cerebrospinal fluid (CSF) examination and electrophysiological tests were superior to CT examinations in identifying and classifying abnormalities [28]. They also suggested that CT imaging could be more prominent in excluding alternative pathologies and assessing the degree of white matter involvement [28].

MRI, as opposed to CT, has become an indispensable tool in diagnosing, treating, and prognostically assessing MS. Current guidelines recommend that every patient newly diagnosed with MS should undergo MRI brain imaging [4]. Additionally, if clinical presentation suggests spinal involvement, imaging should encompass the entire spinal cord [29].

MRI imaging is also a key component of the McDonald diagnostic criteria for MS. These criteria, first introduced in 2001 and most recently revised in 2017, incorporate MRI findings as a fundamental element in confirming an MS diagnosis [30]. This is especially valuable since many diseases mimic the presentation of MS: infectious diseases like Lyme disease and syphilis; vasculitis and other inflammatory conditions like sarcoidosis; genetic conditions such as leukodystrophies; and even brain tumors and other demyelinating disorders such as neuromyelitis optica [31].

The McDonald criteria utilize MRI evidence to establish the dissemination of lesions in both time and space. Table 2 outlines the specific MRI evidence required to meet the McDonald criteria for diagnosing MS.

| What evidence for MS does the patient already have? | What additional data is needed for an MS diagnosis? |
|---|---|
| Two or more relapses **and either** objective clinical evidence of two or more lesions **or** objective clinical evidence of one lesion together with reasonable historical evidence of a previous relapse | None |
| Two or more relapses; objective clinical evidence of one lesion (shows DIT) | One or more MRI detected lesions typical of MS **or** A further relapse showing damage to another part of the CNS |
| One relapse; objective clinical evidence of two or more lesions (shows DIS) | Dissemination in time shown by: Oligoclonal bands **or** MRI evidence of a new lesion since a previous scan **or** A further relapse |
| One attack/relapse; objective clinical evidence of one lesion (known as 'clinically isolated syndrome') | Dissemination in space shown by: One or more MRI detected lesions typical of MS **or** A further relapse showing activity in another part of the CNS Dissemination in time shown by: Oligoclonal bands **or** MRI showing new lesions since a previous examination **or** A further relapse |
| Insidious neurological progression suggestive of multiple sclerosis (typical for primary progressive MS) | Continued progression for one year (from previous symptoms or by ongoing observation) plus any two of: One or more MRI detected lesions in the brain typical of MS, Two or more MRI detected lesions in the spinal cord, Oligoclonal bands in the spinal fluid |

Table 2: Evidence needed to secure an MS diagnosis and the McDonald criteria.

Wattjes et al. acknowledge some criticisms of these criteria, including the omission of clinical tests and the potential to be too lenient for accurate diagnosis, particularly in the presence of ischemic small vessel disease [32].

Since its 2010 revision, the McDonald criteria have allowed a formal diagnosis through a first-time examination demonstrating both dissemination in time and space [32].

In its latest revision in 2017, the McDonald criteria saw some changes compared to its 2010 version, among which are [30]:

- CSF-specific oligoclonal bands now allow the diagnosis of MS in patients with a typical clinically isolated syndrome or MRI evidence of dissemination in space;

- In patients with supratentorial, infratentorial, or spinal cord syndrome, symptomatic lesions can demonstrate dissemination in space or time;
- Cortical lesions can now be considered for the evaluation of dissemination in space.

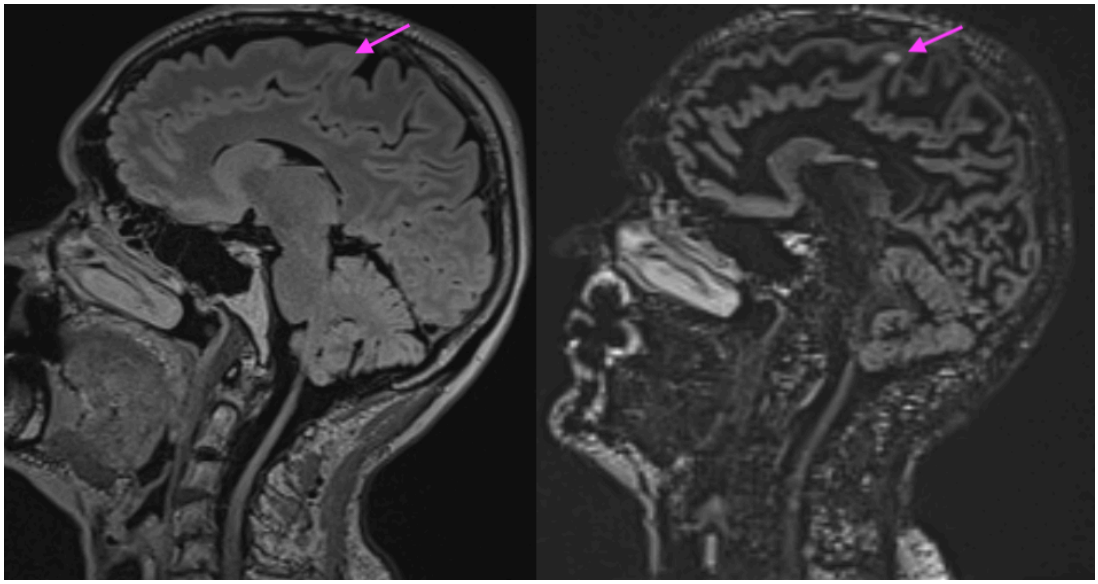

Figure 2: Comparison of a juxtacortical lesion on FLAIR (left) and DIR (right). Sagittal view of a 3D $T_2$-weighted FLAIR sequence (left) and sagittal view of a 3D $T_2$-weighted DIR sequence (right) with pink arrows pointing at the same juxtacortical lesion. The patient is a 54-year-old female with diagnosed RRMS.

### 1.4.2 Current MRI practice in cerebral and spinal MS

Traditionally, MRI in MS has primarily utilized $T_2$-weighted pulse sequences to highlight hyperintense lesions indicative of demyelination and inflammation [33]. This approach remains a fundamental part of brain MRI protocols, coupled with many new sequences over the past decades. One of them is the fluid attention inversion recovery (FLAIR) pulse sequence, which nulls the signal from fluid to suppress the cerebrospinal fluid signal. FLAIR pulse sequences have become increasingly important, particularly for their high contrast in identifying lesions in periventricular and juxtacortical regions [34].

Double inversion recovery (DIR) pulse sequences should also be noted. DIR employs two time inversions to suppress cerebrospinal fluid and white matter signals [35]. Some authors have demonstrated that DIR surpasses FLAIR and $T_2$-weighted TSE in cerebral lesion identification due to its superior lesion-white matter contrast [35,36]. However, newer research suggests that DIR is less effective than 3D phase-sensitive inversion recovery (PSIR) pulse sequences in identifying cortical lesions [37].

MRI developments have also occurred for the spinal cord. The short tau inversion recovery (STIR) is an example. It is a fat-suppression technique that has been shown to be more sensitive than $T_2$-weighted TSE images in identifying spinal MS lesions [26].

Still considering the spinal cord, another pulse sequence that has attracted attention is the PSIR, a $T_1$-weighted sequence combined with phase-sensitive reconstruction. It has been proposed to achieve high lesion-to-cord contrast and lesion-limited definition [26]. A study conducted by Fechner et al., testing a 3D PSIR sequence at 3T for a hundred patients, demonstrated that this pulse sequence could enhance lesion detection in the cervical spinal cord when compared with a standard protocol composed of postcontrast $T_2$-weighted TSE and $T_1$-weighted TSE [26].

The applicability of $T_1$-weighted PSIR sequences, whether 2D or 3D, also extends to the brain. In this regard, the research conducted by Favaretto et al. [37] supports that PSIR pulse sequences are more efficient in identifying cortical brain lesions than DIR. Their work identified over four times more lesions through PSIR sequences than through DIR.

Further advancement came with higher magnetic field strengths. An example is the application of 7T MRI in MS diagnosis and evaluation. 7T MRI enhances the detection of the central vein sign and leptomeningeal inflammation in MS patients and aids in differentiating MS from conditions like neuromyelitis optica spectrum disorders and systemic lupus erythematosus by imaging iron deposits [38]. It should be noted, though, that 7T MRI has yet to be established in the clinical routine. Its limitations include uncomfortably longer scan times and insufficient safety studies for implants and devices [38].

### 1.4.3 The role of contrast-enhanced $T_1$-weighted pulse sequences

Gadolinium-based contrast agents (GBCAs) are frequently added to MRI protocols due to the association between the breakdown of the blood-brain barrier and new lesions [39]. The administration of contrast agents is key in identifying active demyelinating lesions since a disruption in the blood-brain barrier facilitates gadolinium accumulation. This accumulation, in turn, results in increased signal intensity or hyper-intensity observable in $T_1$-weighted MRI images [40].

For several reasons, contrast-enhanced $T_1$-weighted sequences are added to MRI protocols for diagnostic and follow-up purposes. Primarily, the application of contrast agents substantially increases the sensitivity of MRI in diagnosing lesions, particularly smaller ones that may not be discernible in non-contrast-enhanced images [41].

A retrospective analysis conducted by Mattay et al. [39] questions the validity of repeated contrast administration in patients with unconfirmed disease progression. Their study included brain MRIs of 138 patients and concluded that progression could only be confirmed

in 24% of subjects, while every lesion enhancement was associated with new lesions. These authors argued that it should be reasonable to administer contrast only in cases with evidence of progression in unenhanced images.

The use of GBCAs is not without pitfalls or potential side effects. Evidence suggests that gadolinium can deposit in the brain and other tissues like the liver, bones, and skin, raising concerns about its long-term safety [42]. The accumulation of gadolinium in the brain also seems to occur with an intact brain-blood barrier regardless of renal function [42]. Moreover, some patients may exhibit allergic reactions to the contrast material. In this regard, the rate of adverse effects after administering GBCAs lies around 0.07% to 2.4% [43, 44]. Most of these are not life-threatening, however, and most consist of type A, including pain, nausea, vomiting, dizziness, and headaches [43, 44]. Anaphylaxis is observed only in 0.01% of cases [43, 45].

Fechner et al. [26] also acknowledge multiple administrations of gadolinium in young people for the separate imaging of the brain and spinal cord—which is multiplied by the fact that they tend to undergo many scans throughout their lives. Evaluating spinal lesions through highly sensitive sequences, such as the 3D $T_1$-weighted PSIR pulse sequence, could be an alternative.

The 2021 MAGNIMS–CMSC–NAIMS consensus recommendations [46] highlight differences in contrast application protocols for brain and spinal cord examinations. For diagnosing MS, brain MRI protocols recommend axial or 3D sagittal $T_1$-weighted sequences after applying contrast. However, these are optional when assessing disease activity or for monitoring purposes. In contrast, for the spinal cord, post-contrast $T_1$-weighted sequences are recommended solely for diagnosing MS. Outside of this context, contrast is not advised for safety monitoring of disease-modifying treatments and is only considered optional for assessing disease activity.

## 1.5 Hypothesis

Multiple sclerosis, first described in the nineteenth century, is a disease spectrum that has seen improvements in diagnosis and therapy in the past century. With the introduction of MR imaging and, eventually, the McDonald criteria, the diagnostic approach to this condition has become increasingly systematic.

Recent advancements have focused on improving MRI of the spinal cord, a challenging structure due to its technical and anatomical complexities. In this context, $T_1$-weighted PSIR pulse sequences in 3T magnetic fields might be particularly effective, outperforming sagittal post-contrast $T_2$-weighted and $T_1$-weighted sequences in detecting cervical spinal lesions associated with MS [26].

Coupled with this discussion lies the applicability of contrasted-enhanced $T_1$-weighted pulse sequences for disease monitoring, which is deemed optional in the 2021 MAGNIMS–CMSC–NAIMS consensus recommendations [46]. Besides the increasing evidence of gadolinium accumulation and possible toxicity [42], young patients diagnosed with MS currently face the prospect of undergoing multiple contrast injections in the course of their lives [26]. This is also aggravated because brain and spinal cord imaging are frequently performed independently.

Considering this background, our study investigates whether 3D $T_1$-weighted PSIR pulse sequences at 1.5T magnetic field strength can effectively identify demyelinating lesions in the spinal cord in patients with diagnosed RRMS, and whether contrast-enhanced 2D $T_1$-weighted TSE sequences provide significant additional diagnostic information beyond that obtained with PSIR.

# 2 Methods

## 2.1 Ethical considerations

In November 2020, the ethics application with the number D624/20 received a positive vote from the Ethics Committee of the Medical Faculty of the Christian-Albrechts-University in Kiel. This application outlined the prospective assessment of multiple sclerosis patients with clinically indicated MRI examinations at the Clinic for Radiology and Neuroradiology between December 2020 and June 2021. This research has also been conducted according to the ethical standards of the 1964 Declaration of Helsinki and its later amendments.

This research had no external sponsorship, and the researchers involved stated no conflicts of interest.

## 2.2 Study population

The study involved 50 patients with diagnosed RRMS. Patients were included consecutively, and patients with other forms of MS were excluded.

Patient data was collected regarding gender, age, current disability according to the EDSS, and time elapsed since the MS diagnosis. Clinical information about the patient's current therapy regimen was also collected.

## 2.3 MRI equipment and imaging pulse sequences

All MR images were acquired through the same MRI system (1.5T, MAGNETOM Aera, Siemens Healthcare GmbH, Erlangen, Germany). The maximum gradient strength was 45 mT/m.

The syngo software (Versions E11C and E11E, Siemens Healthcare GmbH, Erlangen, Germany) operated the MRI system.

For each patient, we employed a 20-element head coil, a 4-element neck coil, and a 32-element array coil positioned on the upper chest (Siements Healthare GmbH).

Our institution added a 3D $T_1$-weighted PSIR pulse sequence to the routine protocol. Table 3 describes the pulse sequence parameters used in the study.

| Parameters | Pulse sequences | | | | |
|---|---|---|---|---|---|
| | PSIR | STIR | T2-weighted | T2-weighted | CE T1-weighted |
| Slice orientation | sagittal | sagittal | sagittal | axial | sagittal |
| TE (ms) | 194 | 69 | 99 | 99 | 11 |
| TR (ms) | 4000 | 7430 | 4300 | 6830 | 570 |
| TI (ms) | 350 | 170 | - | - | - |
| FA (°) | 120 | 180 | 150 | 150 | 150 |
| Slice thickness (mm) | 1 | 3 | 3 | 3 | 3 |
| Gap between the slices (mm) | - | 0.3 | 0 | 6-7.5 | 0 |
| Matrix (pixels) | 256×224 | 384×384 | 384×384 | 384×384 | 384×384 |
| Field of view (mm²) | 250x219 | 320x320 | 320x320 | 220x220 | 280×280 |

Table 3: Pulse sequence parameters.

No contrast-enhanced $T_1$-weighted TSE pulse sequence was included in the study protocol of patients who refused or whose cases had no clinical indication. The reasons for this varied: two cases had no specified reason for the omission; one patient, who was breastfeeding at the time, chose to avoid gadolinium; another patient had a known allergic reaction to contrast; lastly, it was not possible to place a peripheral IV line on one patient for gadolinium administration.

## 2.4 Image analysis and quality assessment

Three raters with clinical experience spanning three (F. B.N.), ten (M. H.), and twelve (S. P.) years evaluated the datasets retrospectively. The rater with three years of experience is a radiology resident with expertise in neuroradiology, while the other two are board-certified neuroradiologists. All raters were blinded to any clinical information.

Images were divided into three datasets:

- Sagittal 2D $T_2$-weighted TSE images paired with axial 2D $T_2$-weighted TSE images, labeled "$T_2$";
- Sagittal 2D $T_2$-weighted STIR images combined with axial 2D $T_2$-weighted TSE images, labeled "STIR";
- 3D $T_1$-weighted PSIR images, labeled "PSIR".

Each dataset was coupled with sagittal contrast-enhanced 2D $T_1$-weighted TSE sequences. Contrast-enhanced sequences were divided into two sub-stacks: cervical and upper thoracic; middle lower thoracic and medullary cone.

The following figure depicts the cervical spinal cord of the same patient, captured in three different sequences:

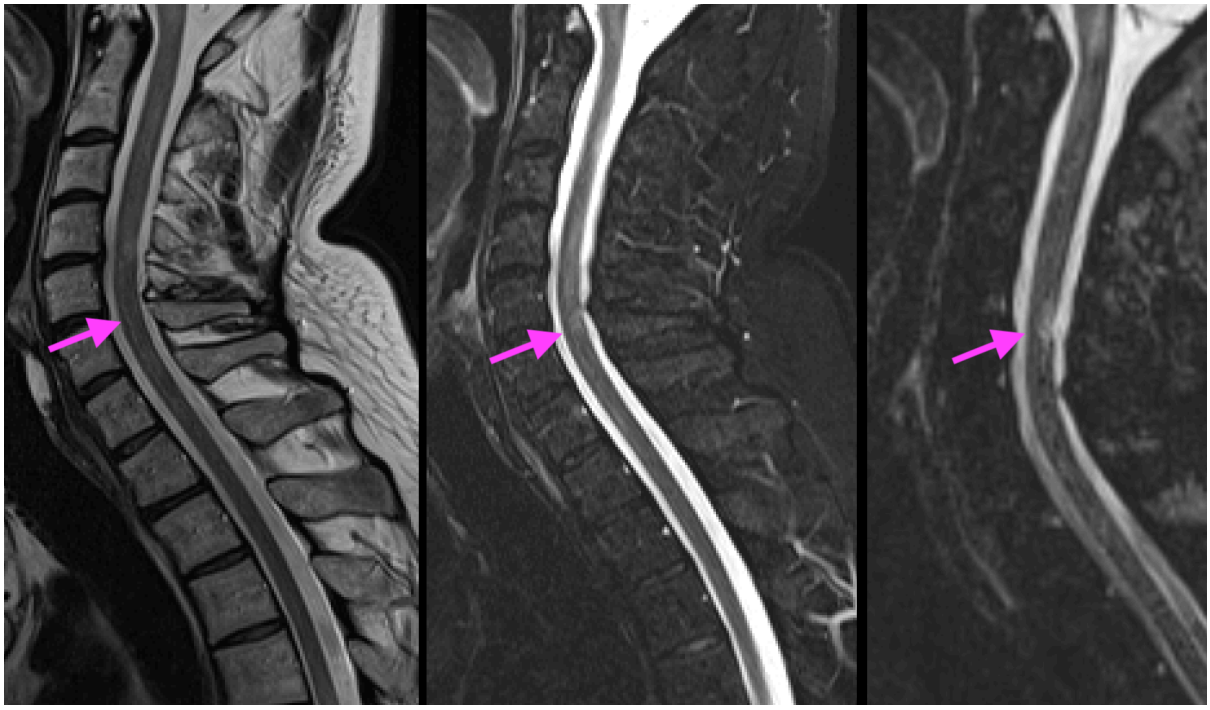

Figure 3: Cervical lesions observed on sagittal $T_2$-weighted TSE (left), sagittal $T_2$-weighted STIR (center), and 3D $T_1$-weighted PSIR (right). The pink arrows indicate a circumscribed hyperintense lesion at the level of the fifth/sixth cervical vertebra. While the lesion is barely visible on sagittal T2-weighted TSE (left), it is recognizable on sagittal T2-weighted STIR (middle) and evident on 3D T1-weighted PSIR (right). This 37 year-old male patient has multiple, confluent lesions of the cervical spine, as observed at the upper cervical levels on STIR (middle) and PSIR (right).

To mitigate memory bias, each dataset was evaluated independently with a minimum interval of six weeks between the assessments of different sets. Additionally, cases were randomized and presented in varying orders for each evaluation.

For the imaging quality assessment, a discrete and arbitrary five-point scale was employed:

- Excellent imaging quality with no artifacts;
- Good imaging quality with minor artifacts but with no hindrance in evaluation;
- Acceptable quality with slight impairment for evaluation;

- Poor imaging quality with significant evaluation obstruction;
- Extremely poor imaging quality, making evaluation infeasible.

| Grading of image quality | Image | Image description |
|---|---|---|
| Excellent image quality. |  | Sagittal $T_2$-weighted TSE image of the cervical spinal cord with no artifacts. |
| Good imaging quality. | 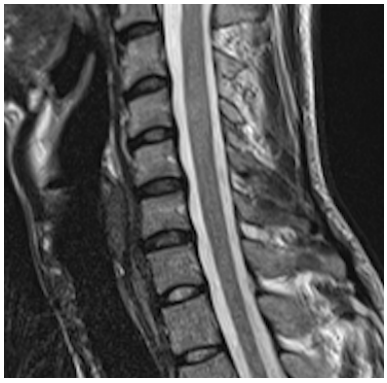 | Sagittal $T_2$-weighted TSE image of the cervical spinal cord with minor artifacts. |
| Acceptable imaging quality. | 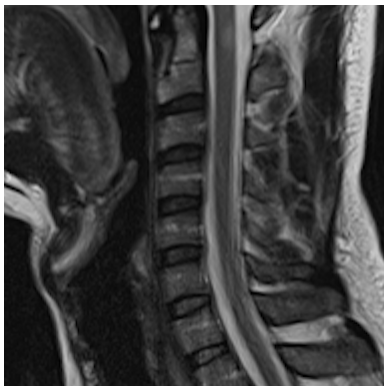 | Sagittal $T_2$-weighted TSE image of the cervical spinal cord with moderate artifacts that slightly impair evaluation. The assessment at the level of the fourth to the seventh cervical vertebra is notably hindered. |

| | | |
|---|---|---|
| Poor imaging quality. |  | Sagittal $T_2$-weighted TSE image of the cervical spinal cord with major artifacts of the whole cervical spinal cord. |
| Extremely poor imaging quality. | 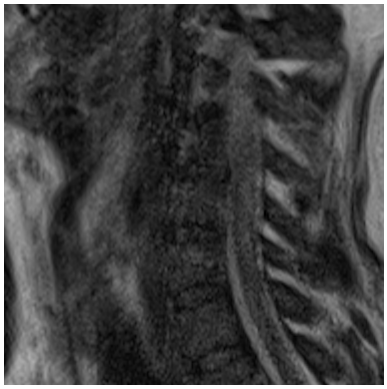 | Sagittal $T_2$-weighted TSE image of the cervical spinal cord with major artifcacts that render the assessment impossible. |

Figure 4. Overview of imaging quality.

This assessment was separately applied to the cervical spinal cord, the thoracic spinal cord, and the medullary cone — in every dataset (“T2 TSE”, “STIR,” and “PSIR”) of every patient.

Each rater was responsible for recording the number of MS lesions, categorizing them based on their location in both the sagittal and axial planes.

For this analysis, the spinal cord in the sagittal plane was segmented into three distinct regions: cervical, thoracic, and medullary cone. Similarly, the axial plane was divided into three areas: lateral, ventral/dorsal, and central (Figure 5).

Upon completing the lesion count at every anatomical site and every dataset, raters gauged their confidence in their evaluations through a three-point scale. This measurement considered the reproducibility of the lesion, whether it was blurry or sharply marginated, and how likely it was to be the byproduct of artifact generation. We assigned no lower threshold for lesion size.

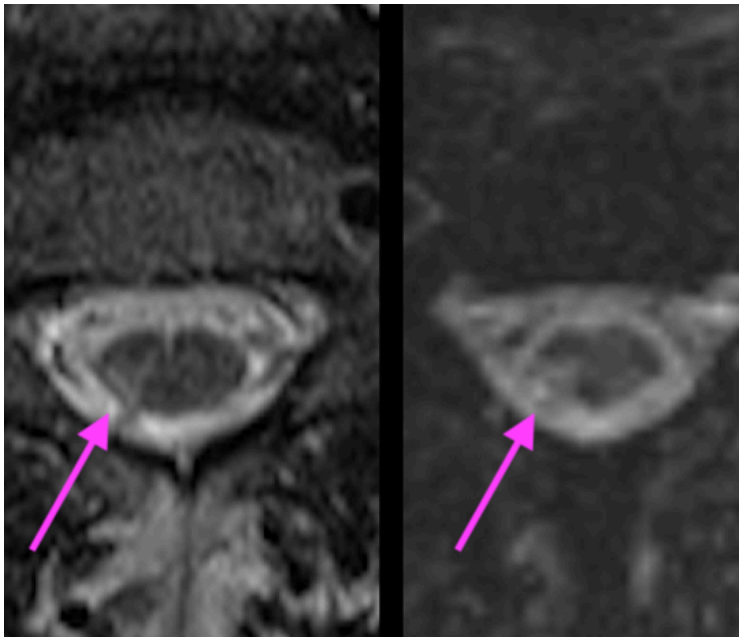

Figure 5: Axial $T_2$-weighted TSE (left) and $T_1$-weighted PSIR (right) images of a lateral cervical lesion. Hyperintense lesions (pink arrow) are recognizable on the right lateral cervical cord on the axial plane. While this lesion is blurry and poorly defined on the $T_2$-weighted TSE sequence (left), it is more prominent on the $T_1$-weighted PSIR (right).

Lesion certainty was numerically evaluated through a three-point discrete scale: certain (1), moderate (2), and uncertain (3).

A technical measurement ensued: the lesion-to-cord contrast ratio (CR lesion/cord), computed using the following formula where:

- CR is the lesion-to-cord contrast ratio;
- signalLesion is the average signal of the ROI measurement of an affected area;
- signalCord is the average signal of the ROI measurement of an unaffected area of the same spinal level;

$$CR = (signalLesion - signalCord)/signalCord$$

In this analysis, regions of interest (ROI) were manually outlined in the sagittal plane across the cervical, thoracic, and medullary cone segments for each dataset ("$T_2$ TSE," "STIR," and "PSIR"). The largest lesion was selected for measurement whenever a lesion was identified in any of these segments. This measurement was then compared to the surrounding tissue unaffected by lesions.

The same formula was applied to each sequence.

Figure 6 illustrates the ROI measurement of a cervical lesion:




Figure 6: ROI measurements of the same cervical lesion in the sagittal plane on $T_2$-weighted STIR (left) and $T_2$-weighted TSE (right). This figure compares the contrast between the same lesion and the surrounding unaffected tissue in a 2D $T_2$-weighted TSE sequence and in a 2D $T_2$-weighted STIR sequence based on a semi-quantitative circular ROI.

Lastly, the most experienced radiologist (S.P.) performed a consensus reading to determine the ground truth, which included all pulse sequences, the clinical history, and the results from the previously blinded readings.

## 2.5 Analysis of contrast-enhanced 2D $T_1$-weighted TSE sequences

2D $T_1$-weighted TSE images were obtained after intravenous injection of a gadolinium-based contrast agent (0.1 mmol/kg Gadobutrol).

Raters evaluated each spinal level in the datasets ("$T_2$ TSE," "STIR," and "PSIR"), comparing them to the corresponding contrast-enhanced sagittal 2D $T_1$-weighted TSE sequence. If this comparison revealed visible lesions, those lesions were then compared to those identified in the respective dataset to determine if new clinical information was provided.

### 2.6 Statistical analysis

The statistical analysis was carried out using the Jamovi project's dedicated statistical software (jamovi version 2.2.5; available at www.jamovi.org).

The Shapiro-Wilk test was conducted to assess normality in the distribution. Given the distribution's asymmetry, the median and the range were used to describe the age of the patients, the EDSS scores, and the duration between the diagnosis of MS and the MRI scan.

For testing the interrater agreement of lesion count, we employed the interclass correlation coefficient (ICC). In this regard, values over 0.9 indicated excellent agreement, the range 0.75-0.9 indicated good agreement, and the range 0.5-0.74 was associated with moderate agreement. At last, values under 0.5 indicated poor agreement [47].

The Wilcoxon rank-sum test, which is a nonparametric test for two populations with independent sampling, evaluated the contrast ration lesion-cord. In this regard, a p-value $< 0.05$ was deemed statistically significant.

The Spearman’s rank correlation coefficient evaluated the correlation of spinal cord lesions and the EDSS: 1.0 was considered a perfect correlation; 0.8-0.99 very strong; 0.6-0.79 moderate; 0.3-0.59 fair; 0.1-0.29 poor; 0-0.09 no correlation [48].

# 3 Results

## 3.1 Population

Of the 50 patients studied, a significant gender difference was noted: 70% were female.

The mean age of the participants was 39.4 (with a standard deviation of 12). The youngest participant was 23, while the oldest was 72 at the time of the study.

Concerning the time elapsed between the MS diagnosis and the MRI examination enrolled in the study, a considerable difference was observed between the patients. This spectrum varied from 0 (the examination was coupled with the formal diagnosis) to over 20 years. On average, slightly over 58 months elapsed from the MS diagnosis to when the MRI examination was undertaken.

In terms of the degree of clinical disability, subjects presented with an average EDSS of 2.06.

The table below summarizes the recorded statistics regarding patient age, clinical disability measured in EDSS, and time elapsed between the clinical diagnosis and the study MRI:

| | Mean ± SD | Minimum | Maximum |
|---|---|---|---|
| **Age (years)** | 39.44 ± 11.98 | 23 | 72 |
| **EDSS (points)** | 2.06 ± 1.62 | 0 | 6 |
| **Time elapsed between diagnosis and MRI (months)** | 58.8 ± 67.3 | 0 | 249 |

Table 4: Population data of the present study.

Regarding current medication and MS therapy regimen, 40% of the subjects were not taking any medication at the time. Ocrelizumab, a drug that selectively depletes CD20+ B cells through cytotoxicity, antibody-dependent cellular phagocytosis, and apoptosis [49], represented the most common therapy regimen — administered to 30% of patients. A smaller percentage of subjects (16%) were administered dimethyl fumarate, while teriflunomide was the preferred treatment for just 4% of patients. Only 2% were prescribed interferon beta1a or glatiramer acetate as their therapy of choice. The following figure illustrates the distribution of drug use within the study population:

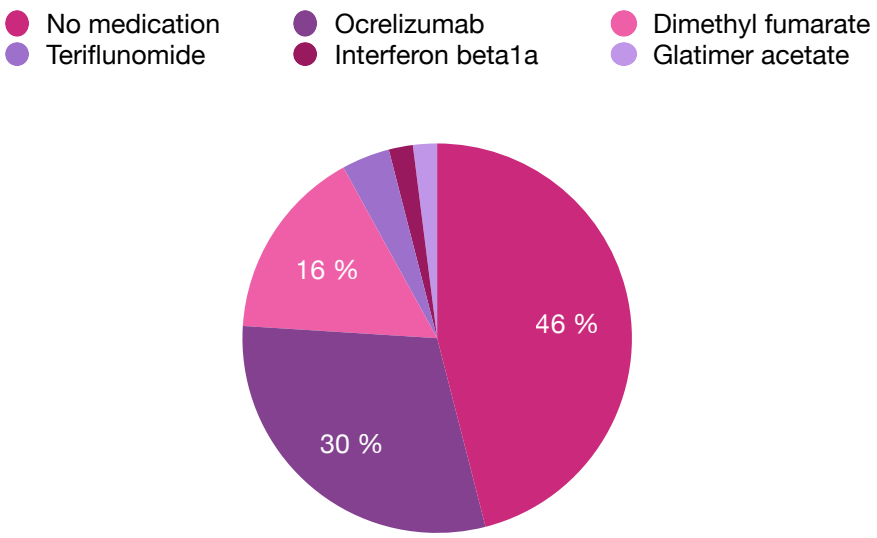


Figure 7: Current therapy regimens in the study population. Almost half of the study patients were taking no medication during the time of the study. Of those who were taking medication, over the half were being administered ocrelizumab.

### 3.2 Lesion count and distribution

The first rater (S.P.), who had the most experience in neuroradiology, identified the highest number of lesions in any given dataset (348 in the PSIR set), which was notably higher than the number of lesions observed in the $T_2$ (146) and STIR (175) sets for this rater.

The results assembled by the second rater (M.H.), who had 8 years of neuroradiology experience, followed a different trend. The maximum number of lesions was observed in the $T_2$ dataset (158), and this represents only a marginal increase in comparison to the STIR (138) and PSIR (137) datasets.

The third rater (F.B.N.), a resident with a three-year experience in neuroradiology, reported lesion counts that also differed from the other two radiologists. This observer reported 216 lesions in the PSIR sequence, a higher count than reported in the $T_2$ (175) and STIR (166).

These values are depicted in the table below:

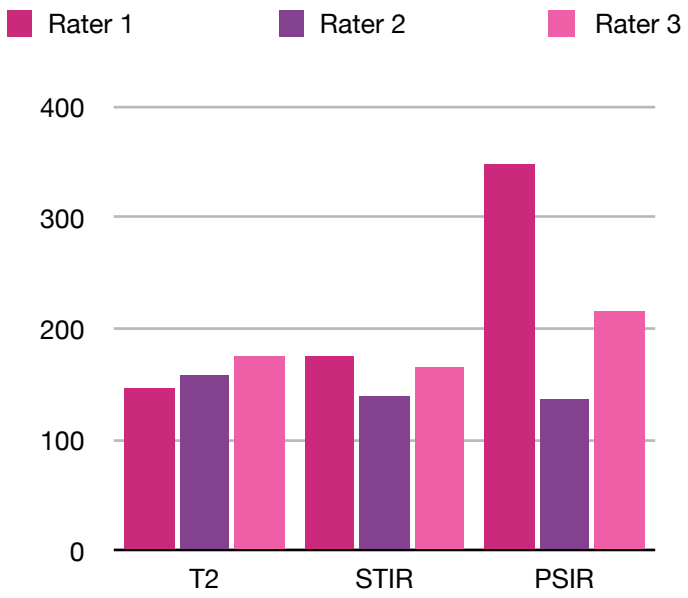


Table 5: Lesion count according to pulse sequence and rater.

The agreement between raters on lesion counts varied by data set:

PSIR: Good agreement (ICC 0.64)

STIR: Excellent agreement (ICC 0.82)

$T_2$ TSE: Substantial agreement (ICC 0.74)

In the consensus reading to determine the ground truth, 239 lesions were detected, making the average lesion count 4.78 per patient. About variability, one patient had as many as 22 lesions, while seven patients had none.

The number of lesions positively correlated to the EDSS ($r = 0.31$; $p = 0.03$) was assessed through Spearman's rank correlation coefficient.

The segmental analysis of the anatomical distribution of lesion count evidenced that over half of the lesions (131; 54.8%) affected the cervical spinal cord, while over forty percent (101; 42.3%) were identified in the thoracic spinal cord. Only a few lesions (7; 2.9%) involved the medullary cone.

The figure below illustrates the lesion distribution in the sagittal plane:

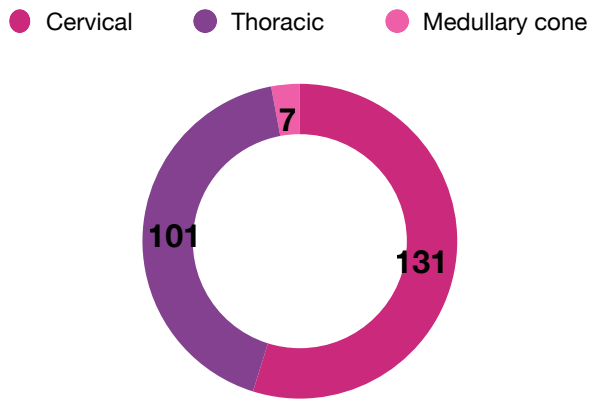


Figure 8: Anatomical distribution of lesions (sagittal plane).

Lesions were further analyzed according to their locations in the axial plane, and it was shown that 52.3% of lesions were located in the lateral spinal cord, 28.9% of lesions were located ventrally or dorsally in the spinal cord, while 18.8% had a central location. This can be observed in the following figure:

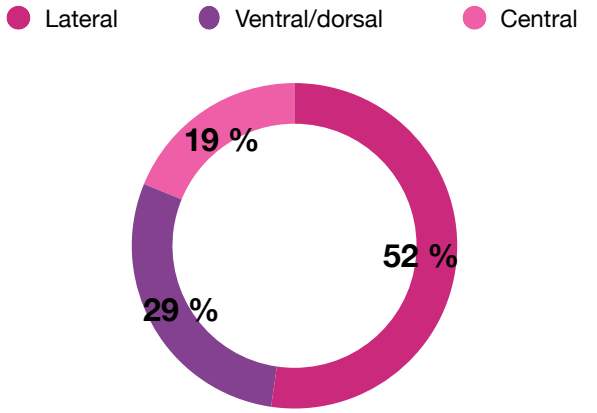


Figure 9: Anatomical distribution of lesions (axial plane).

### 3.3 Imaging Quality Assessment

Table 9 depicts the mean imaging quality according to the proposed scale for image assessment:

| | Cervical imaging quality | Thoracic imaging quality<br><br>Mean ± SD | Imaging quality of the medullary cone |
|---|---|---|---|
| PSIR sagittal | 1.95 ±0.81 | 2.2 ±0.77 | 2.1 ±1.1 |
| STIR sagittal | 1.69 ±0.82 | 1.77 ±0.65 | 1.29 ±0.03 |
| T2-weighted sagittal | 1.47 ±0.78 | 1.57 ±0.66 | 1.39 ±0.6 |
| T2-weighted axial | 1.96 ±0.94 | 2.19 ±0.66 | 1.64 ±0.82 |
| $T_1$ CE sagittal | 1.33 ±0.53 | 1.19 ±0.44 | 1.4 ±0.64 |

Table 6: Analysis of the imaging quality of the different sequences is demonstrated for the cervical spinal cord, the thoracic spinal cord, and the medullary cone.

### 3.4 Lesion detection rates

In sagittal and axial $T_2$-weighted TSE images, 59.9% of cervical lesions were detected, which occurred for 59.5% of the thoracic lesions. In the sagittal $T_2$-weighted STIR combined with axial $T_2$-weighted images data set, cervical lesions were detected in 58.6% of cases, while 59.1% of thoracic lesions were identified. As for PSIR images, cervical lesions were detected in 77.1% and thoracic lesions in 72.6%. These findings are displayed in Figure 10.

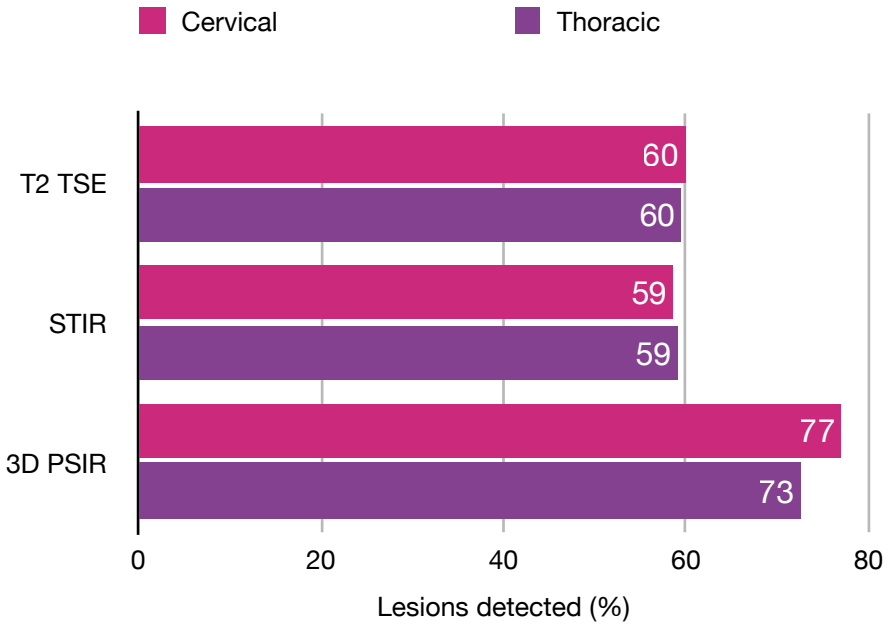


Figure 10: Lesion detection rates in different imaging techniques.

False positive rates were observed as follows for each dataset:

- $T_2$: 17.7 per rater;
- STIR: 13 per rater;
- PSIR: 43.7 per rater.

### 3.5 Lesion-to-cord contrast ratio (CR) analysis

| | 2D T2 TSE | 2D T2 STIR | 3D T1 PSIR |
|---|---|---|---|
| Cervical | 0.29 ± 0.15 | 0.44 ± 0.21 | 0.95 ± 0.4 |
| Thoracic | 0.26 ± 0.15 | 0.44 ± 0.25 | 0.88 ± 0.5 |
| Total | 0.28 ± 0.15 | 0.44 ± 0.23 | 0.92 ± 0.45 |

Table 7. Lesion-to-cord contrast ratio values for each imaging dataset and spinal segment.

The differences between the contrast ratios of the different imaging datasets were deemed significant for both the cervical and the thoracic segment and for both regions analyzed together as well (each $p < 0.001$). It is important to note that the STIR-CRs were higher than those observed in the 2D $T_2$ TSE group ($p < 0.001$).

### 3.6 Certainty of lesion count

The average certainty of lesion count and the standard deviation are depicted in Table 12 and categorized by anatomical region: cervical, thoracic spinal cord, and medullary cone. The average certainty of the locations taken together (total) is also included. The different imaging techniques showed no marked differences in certainty of lesion count.

| | PSIR | 3D STIR | $T_2$ TSE |
|---|---|---|---|
| | | Mean ± SD | |
| Cervical | 1.36 ± 0.62 | 1.39 ± 0.62 | 1.36 ± 0.61 |
| Thoracic | 1.44 ± 0.65 | 1.37 ± 0.59 | 1.54 ± 0.64 |
| Conus | 1.1 ± 0.36 | 1.06 ± 0.3 | 1.13 ± 0.44 |
| Total | 1.34 ± 0.6 | 1.27 ± 0.54 | 1.34 ± 0.6 |

Table 8: Certainty of lesion count.

### 3.7 Contrast-enhanced 2D $T_1$-weighted TSE sequences

45 subjects underwent an MRI with intravenous GBCA as per the institution’s protocol.

All raters agreed that the contrast-enhanced $T_1$-weighted pulse sequences did not provide extra information in any of the cases across all datasets. Figure 11 compares a $T_2$-weighted sequence with a contrast-enhanced $T_1$-weighted pulse sequence from the same patient:

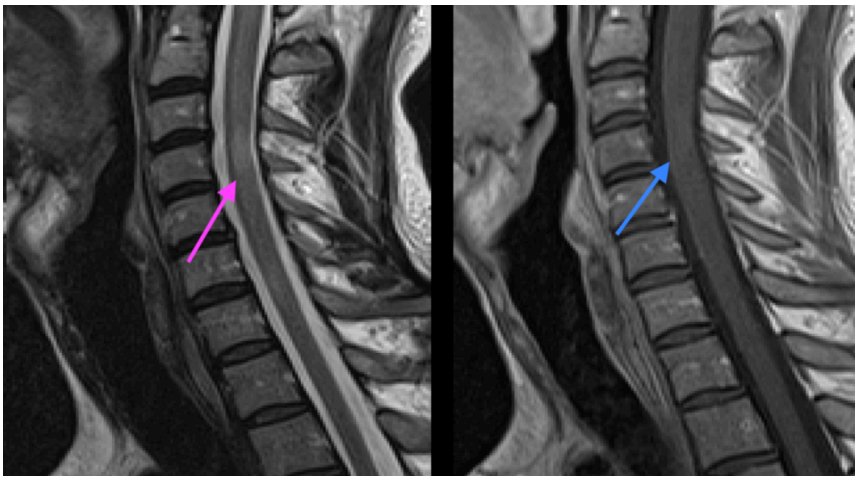

Figure 11: Comparison of a 2D $T_2$-weighted TSE (left) and 2D gadolinium-enhanced $T_1$-weighted TSE sequence (right) of the same patient. On the left, a well-defined and oval-shaped lesion is seen at the level of the third and fourth cervical vertebra in the sagittal plane of a $T_2$-weighted sequence (pink arrow). On postcontrast $T_1$-weighted TSE, the lesion is barely identifiable (blue arrow).

# 4 Discussion

## 4.1 Population

Multiple sclerosis is a condition predominantly affecting younger individuals, yet it encompasses a diverse patient demographic across different backgrounds and ethnicities. It is crucial to consider this heterogeneity when selecting a representative population for studies on MS.

Our study cohort's age and disease stage characteristics aligned well with the existing literature. For instance, our study group comprised 35 female patients, 70% of the total participants. This proportion closely mirrors the statistics in The Atlas of MS, which reports that 73% of MS patients are female [7]. In terms of age demographics, our study population had a mean age of 37 years, closely aligning with the mean age of 33 years reported in The Atlas of MS [7]. Such similarities underscore the representativeness of our study group in reflecting the broader MS patient population.

Regarding the degree of disability, we employed the EDSS scale to assess each patient's current impairment. By including patients in different stages of spinal and cerebral involvement with EDSS points ranging from 2 (defined as minimal disability) to 6 (assistance required to walk and work), we minimized possible biases arising from only including patients with a determined progress level in the disease.

About the EDSS scale and lesion count, it is relevant to note that a clinical-radiological paradox has been described in the setting of multiple sclerosis follow-up, defined as a mismatch between radiological lesions and clinical disability [50]. A study by Nij Bijvank et al. showed that such a paradox occurred in a fourth of the investigated patients [50], even if, compared with our study, theirs was not limited to patients with a relapsing-remitting course.

Nij Bijvank et al. offer two explanations for the clinical-radiological paradox [50]. The first suggests that the paradox arises when more radiological lesions are identified than clinically expected, potentially due to the brain's ability to adapt to injury and mask symptoms, a phenomenon referred to as cortical plasticity [50-52]. The second explanation considers that fewer lesions are detected on MRI than would be predicted based on clinical examinations. This discrepancy could result from hidden white matter lesions or not fully utilizing the capabilities of multimodal MRI techniques [50,53,54].

Incorporating a highly sensitive 3D $T_1$-weighted PSIR pulse sequence to study protocols might improve the alignment between clinical symptoms and MRI findings. Supporting this, our research found that the detection of lesions with the 3D $T_1$-weighted PSIR technique was over 10% higher than with traditional $T_2$-weighted TSE and STIR methods for both cervical and thoracic spinal regions. While our results are based on a 1.5T magnetic field strength, they mirror those of Fechner et al. at 3T for the cervical spine [26].

We observe a high variation among the subjects regarding the elapsed time between the MS diagnosis and the MRI examination. This occurred because the time elapsed was not a criterion of exclusion, and patients with recently diagnosed MS and long-standing disease were enrolled.

Furthermore, we focused on patients with RRMS and excluded other forms. This design decision limited the applicability of our findings to this particular disease pattern but helped reduce potential biases that could arise from the inclusion of different disease courses. This approach contrasts with the study design by Fechner et al. [26], in which a broader patient group was evaluated: out of a hundred patients, 82 had RRMS, 12 had secondary progressive MS, and 6 had primary progressive MS. Even if some authors argue against dividing MS into supposedly artificial subgroups [4], including all disease courses in the same research could lead to omitted-variable biases and confounding biases.

### 4.1.1 Drug regimens

Among those on disease-modifying therapies, ocrelizumab, the first humanized anti-CD20 monoclonal antibody to receive approval in the United States [49], was the most commonly prescribed medication used by 30% of the patients, and over half of the patients who were

currently under any pharmacological therapy. This might have been because ocrelizumab tends to be well tolerated and highly efficient in delaying the disease progression of MS [49].

Teriflunomide, an immunomodulatory agent, was the therapy of choice of a smaller patient subset (4%). Acting as a reversible inhibitor of dihydroorotate dehydrogenase and both as an immunomodulator, teriflunomide is currently approved in the US (in the once-daily dosages of 7 and 14mg) and in the European Union (14mg) for RRMS [55].

Both interferon beta1a and glatiramer acetate, long-standing treatments for relapsing forms of MS, were the therapy of choice for 2% of patients. Their reduced usage in our cohort could be attributed to the emergence of newer therapies or possibly side effect profiles compared to newer agents.

## 4.2 Diagnosis and disease monitoring through the 3D $T_1$-weighted PSIR technique

3D $T_1$-weighted PSIR sequences have been examined to identify and monitor both brain and spinal lesions.

Regarding the brain, this sequence has shown a higher signal-to-noise ratio, intensity, and gray-white matter contrast than DIR sequences — improving cortical lesion detection and classification of lesions over DIR in cross-sectional imaging [34,56,57]. As an illustration, Sethi et al. [57] examined 60 MS patients and 30 healthy controls in a 2012 research to compare DIR and PSIR detection rates at a field strength of 3T. On PSIR, these researchers counted at least one intracortical lesion in every MS patient and only one control; on DIR, at least one intracortical lesion was found in 50 of the 60 MS patients and five of the 30 healthy controls. It's important to note that although PSIR provided higher accuracy for both affected and healthy subjects, it required significantly longer scan times (11 minutes compared to 4 minutes for DIR). In clinical settings, where scan times are critical for managing radiology clinic workflows, the fact that PSIR sequences take almost three times longer than DIR sequences could be a drawback. This may hinder the adoption of PSIR in institutional protocols for studying the brain.

For brain imaging, FLAIR sequences are still widely more applied than DIR or PSIR — which have been considered optional sequences in the 2021 MAGNIMS/NAIMS consensus recommendations [46].

Regarding the spinal cord, Fechner et al. [26] have demonstrated that 3D $T_1$-weighted PSIR is a promising sequence to be included in MS protocols at 3T. This working group observed that both detection rates and reading confidence were higher for 3D $T_1$-weighted PSIR images than for the conventional sequences (sagittal postcontrast $T_2$-weighted TSE and $T_1$-

weighted TSE). Their findings, however, were limited to 3T magnetic field strength and the cervical spinal cord. Our study aimed to assess these outcomes when applied to a field strength of 1.5T and the whole spinal cord and confirms that 3D $T_1$-weighted PSIR shows superior outcomes.

### 4.2.1 Inter-rater variability

Variability in interpreting the EDSS and functional parameters in patients with MS can be considerable, especially among physicians with less experience [58]. This variability highlights the impact of inter-rater reliability on MS treatment decisions, independent of radiological findings. To address this potential issue, the research by Fechner et al. [26] and our study included a mix of raters comprising radiology residents and board-certified radiologists. This strategy was designed to account for potential differences in interpretation arising from varied levels of clinical experience.

Our study calculated the inter-rater agreement for the total reported lesions in each dataset ("$T_2$ TSE," "STIR," and "PSIR"). 2D $T_2$-weighted STIR sequences showed excellent agreement (ICC 0.82), while 3D $T_1$-weighted PSIR and 2D $T_2$-weighted TSE images were also associated with good and substantial agreement (ICC 0.64 and 0.74), respectively. These figures support the consistency of lesion identification among raters. These findings also echo those reported by Fechner et al. [26], whose inter-rater and intra-rater agreement were good for both the 3D $T_1$-weighted PSIR and conventional data sets.

It should be noted, however, that the lesion count still varied considerably. The second rater found more lesions in $T_2$-weighted pulse sequences than in the PSIR dataset. In contrast, the PSIR dataset was associated with the biggest lesion count for the two other raters. Further differences among raters might also be observed: while the most experienced rater reported more lesions in the STIR pulse sequence than in the $T_2$ TSE dataset, the opposite happened for the least experienced one. It might be assumed, then, that even though the inter-rater agreement hinted at the reliability of these methods, some relevant differences exist in the analyses of different radiologists.

Inter-rater variability can stem from several sources, with the experience level of each rater being a relevant factor. This can significantly affect their capability to identify and disregard imaging artifacts. The MAGNAMIS/NAIMS consensus [46] suggests including two sagittal sequences to minimize the impact of artifacts. Additionally, our methodology did not specify a minimum lesion size for inclusion, representing another potential source of variability.

### 4.2.2 Lesion detection and interpretation

We found a higher sensitivity with 3D $T_1$-weighted PSIR images than with $T_2$-weighted datasets for lesion detection in the cervical, thoracic, and medullary cone regions. This is consistent with the findings of Fechner et al. [26] at 3T. A possible explanation for this higher detection rate might be the increased resolution of the 3D PSIR images compared with 2D PSIR images, even if Shayganfar et al. recorded the 2D PSIR images in two different planes to compensate for this limitation [59].

It must also be noted that even the 3D $T_1$-weighted PSIR subset missed a considerable amount of lesions compared with the ground truth (77.1% of the cervical lesions and 72.6% of the thoracic ones were identified). A final evaluation by the most experienced rater employed clinical history, prior scans, and all available sequences to establish the ground truth. Several factors could explain this “gap” between readings and the ground truth. For one, raters were blinded to any clinical history. Raters also didn’t have access to prior scans, which could have made identification of smaller, blurry lesions harder. Lastly, this “gap” underscores the value of comprehensive protocols that include multiple sequences.

Our study described higher false positive rates in the PSIR dataset. Compared with the $T_2$-weighted datasets, this increase might be explained by areas of high signal that do not correspond to MS lesions being wrongly tagged. Motion artifacts and underlying tissues might also promote heterogeneities in the spinal signal, leading to incorrect interpretations. Furthermore, the lack of an agreement on minimum lesion size and including blurry lesions likely contributed to these false positive ratios.

Considering these false positive ratios, our focus extended beyond the analysis of 3D $T_1$-weighted PSIR. While this technique might be valuable, it should not be employed in isolation. Instead, 3D $T_1$-weighted PSIR sequences should be integrated into a broader, more comprehensive imaging protocol for the spinal cord that could offset its tendency to yield more false positives.

Our research extends upon studies that have indicated the effectiveness of the 3D $T_1$-weighted PSIR technique in assessing the cervical spinal cord using 3T MRI [26,57,60,61]. Uniquely, ours is the first study to investigate using 3D $T_1$-weighted PSIR at a lower magnetic field strength of 1.5T. Contrasting with the results obtained using 3T MRI [26], though, we did not observe an increased interrater correlation at 1.5T. In our research, the highest level of interrater agreement was found using the 2D $T_2$-weighted STIR technique.

The difference in findings between previous studies using a 3T magnetic field strength and our current study at 1.5T may be attributable to the magnetic field strength. Lesions identified on 3D $T_1$-weighted PSIR may be more easily recognized or reliably detected at 3T than 1.5T. This hypothesis is supported by the notion that higher magnetic field strengths generally

provide greater image clarity and spatial resolution [38]. Currently, no research directly compares the effectiveness of 3D $T_1$-weighted PSIR imaging at these two different field strengths in the same patient population.

The discrepancy between our findings at 1.5T and previous studies conducted at 3T could also stem from methodological differences, particularly regarding the lesion threshold criteria. In our study, no lesion was excluded based on size and sharpness, potentially leading to smaller and blurrier lesions being counted. In contrast, Fechner et al. specifically advised against counting lesions in areas heavily affected by artifacts and recommended only including clear and well-demarcated lesions [26]. This difference in lesion inclusion criteria, combined with the lower magnetic field strength of 1.5T in our study, could explain the higher incidence of false positive lesions we observed, a phenomenon not reported by Fechner et al. [26].

As an illustration, the following figure depicts both a blurry and a circumscribed spinal lesion:

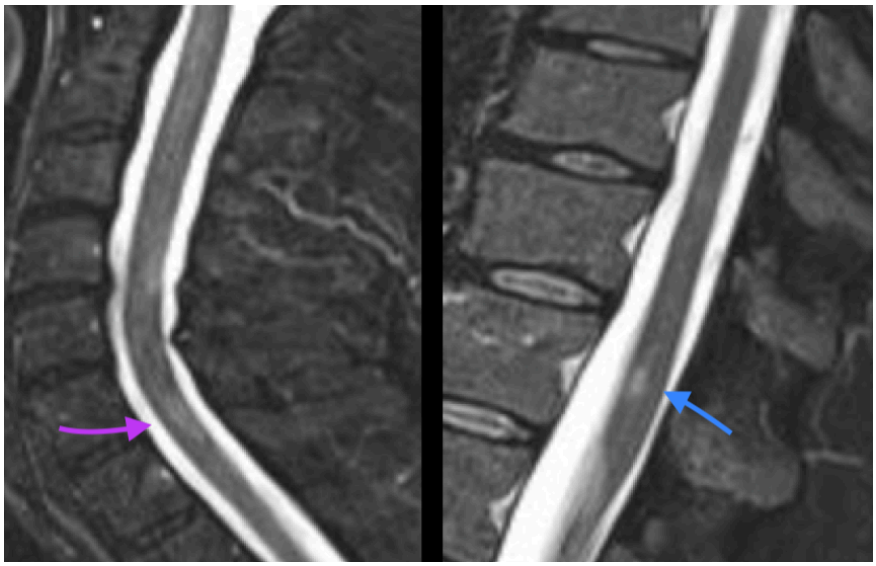

Figure 12. Blurry versus well-defined lesions on 2D $T_2$-weighted STIR images. Sagittal images of two patients at different spinal levels depicting lesions with varying degrees of bluriness. While the image on the left (at cervical level) shows a blurry, poorly delimitated lesion (purple arrow), the picture on the right (at medullary cone level) presents a circumscribed, well-delimitated lesion (blue arrow).

The enhanced detection rate observed with 3D $T_1$-weighted PSIR images might be attributed partially to including small, blurry lesions. The McDonald criteria, intended for MS diagnosis rather than follow-up evaluations, suggest a minimum lesion size of 3 mm to improve specificity and reduce false positives [46]. However, it's essential to recognize that in clinical

practice, MS lesions in the spinal cord can be smaller than 3 mm [30]. Given the spinal cord's relatively small diameter and the proximity of functionally important structures, even small lesions have clinical significance, particularly for differential diagnosis in patients not yet diagnosed with MS.

The MAGNIMS and NAIMS working groups recommend at least two sagittal images to diagnose MS lesions [46]. It is worth noting that in these consensus recommendations, PSIR images are described as optional, primarily due to the current lack of extensive data and clinical experience.

Research regarding the potential benefits of MS imaging in 7T has also been scarcely addressed [38]. This might indicate a direction for future endeavors, even if there are still safety and instrumental barriers to the clinical applicability of 7T MRI.

### 4.2.3 Clinical applicability

Our research suggests that combining 3D $T_1$-weighted PSIR and 2D $T_2$-weighted STIR may be most effective for identifying spinal lesions. This aligns with existing literature suggesting that STIR images are superior to $T_2$-weighted TSE images at 1.5T and 3T [30,46,62].

Studies focusing on the thoracic spine and employing $T_1$-weighted PSIR pulse sequences have provided further insights into this technique’s efficiency at different magnetic field strengths. 2D $T_1$-weighted PSIR sequences at 3T were shown to have lower sensitivity in lesion detection than $T_2$-weighted images [63]. However, when using a 3D $T_1$-weighted PSIR sequence at 3T, detecting lesions in the upper thoracic segments appeared more reliable [60]. Notably, the study cited did not encompass the entire spinal cord.

Our findings indicate that using a 3D $T_1$-weighted PSIR pulse sequence at 1.5T may improve the detection of spinal cord lesions. This is noteworthy because 1.5T MRI systems are more commonly available in clinical settings.

The enhanced performance of 3D $T_1$-weighted PSIR images at 3T, attributed to higher contrast ratios and resolution [57,60], is mirrored in our research at 1.5T. We observed higher contrast ratios in lesions relative to the spinal cord in the PSIR dataset compared to $T_2$-weighted images.

## 4.3 The use of gadolinium in spinal studies of patients with confirmed MS

Contrast-enhanced MRI techniques for the evaluation of patients with confirmed MS who are not experiencing acute symptoms continue to be debated. This concern is amplified by the

potential for gadolinium to deposit in the brain and other tissues, even when the brain-blood barrier is intact and renal function is normal [43]. Additionally, the long-term impacts of these gadolinium deposits remain uncertain [43].

Contrast-enhanced sagittal $T_1$-weighted TSE pulse sequences did not offer any clinical benefit in our research. This finding is echoed by Mattay et al. [39], who propose that contrast should be considered only after disease progression has been confirmed. For spinal cord assessments, the MAGNIMS-NAIMS consensus guidelines [46] recommend applying contrast only when diagnosing MS. In disease monitoring, using contrast-enhanced $T_1$-weighted TSE sequences is optional.

### 4.4 Limitations

This study, which examined lesion detection rates in spinal MS and assessed the use of GBCAs in already diagnosed individuals, involved a modest cohort of 50 patients. While this size allowed for a detailed evaluation of each case, it also presented limitations. A larger cohort could have captured a wider range of disease manifestations, potentially enhancing the external validity of our findings. Notably, our study excluded patients with non-relapsing-remitting MS, limiting our results' scope and applicability.

The study also faced challenges regarding inter-rater variability. Despite showing moderate to good correlation across the assessed techniques, variability may have been influenced by the inclusion of blurred lesions and the absence of a size threshold for counting lesions. Our methodology differed from existing studies, such as one with a 3T field strength that counted only distinct lesions [26], potentially affecting the consistency of our lesion count and inter-rater agreement.

The experience level of raters also warrants consideration. They had significantly differing experience levels, which likely influenced the accuracy of lesion counts and the rate of false positives. In contrast to a similar study [26] that employed a senior and a junior radiologist, our study excluded radiologists lacking specialized neuroimaging expertise. This decision may limit the applicability of our results to settings that do not have access to neuroradiology specialists.

The measurement of ROI lacked standardization, which may have impacted our findings. We compared lesion areas to regions of the spinal cord that appeared unaffected but without established standards for the placement or size of these ROIs. This lack of predefined criteria for ROI placement, both in terms of spatial location and area size, potentially led to variability in the calculated CR values. To enhance the accuracy and consistency of future research, it's essential to establish and adhere to specific parameters for ROI size and location before the commencement of data analysis.

We employed a relatively wide gap in the axial $T_2$-weighted images to reduce total scan time. This decision, however, presents a limitation in lesion detection capabilities. Although axial imaging is considered optional according to international imaging guidelines [46], it might increase detection rates and mitigate false positives, especially considering smaller lesions. In this regard, the MAGNIS/NAIMS consensus recommends a slice thickness of up to 5 mm without a gap [46], compared to the 3 mm thick slices used in our current study.

# 5 Summary

Multiple sclerosis, originally reported in the nineteenth century, is an immune-mediated chronic inflammatory disease that affects both the brain and spinal cord. Due to its unique epidemiology, it poses a significant social and economic burden. Today, despite advancements in treatments and diagnostic tools, identifying inflammatory lesions in the spinal cord remains a challenge. This difficulty is largely due to motion artifacts from adjacent tissues, the spinal cord's distinct geometry, and instrumental variables such as lesion resolution at different magnetic field strengths.

Our study focused on the challenges of detecting spinal inflammatory lesions, highlighting the potential of 3D $T_1$-weighted PSIR at a 1.5T field strength. Building on the findings of Fechner et al. [26] at 3T, we analyzed lesion detection rates in 50 patients diagnosed with RRMS. We divided spinal cord MR images into three datasets, labeled $T_2$ TSE, PSIR, and STIR. Each dataset was paired with sagittal images of contrast-enhanced 2D $T_1$-weighted TSE sequences. We then categorized lesion counts into sagittal and axial planes and measured the confidence of three raters using a discrete scale.

Moreover, we evaluated the relevance of contrast-enhanced sagittal 2D $T_1$-weighted TSE pulse sequences in patients with established RRMS to determine if contrast injection provided significant additional information.

3D $T_1$-weighted PSIR imaging showed higher lesion detection rates than 2D $T_2$-weighted TSE and 2D $T_2$-weighted STIR, echoing previously reported findings at 3T [26]. The inter-rater agreement for 3D $T_1$-weighted PSIR images was comparable to other datasets but had a higher rate of false positives. Additionally, contrast-enhanced 2D $T_1$-weighted TSE images did not provide further clinical information.

The high detection rates with 3D T1-weighted PSIR imaging technique suggest that it holds promise for spinal cord imaging protocols. Our results indicate its potential value at 1.5T, supporting previous findings at 3T. In clinical practice, combining multiple sequences for lesion interpretation is standard, which could mitigate the higher false positive rates seen in 3D $T_1$-weighted PSIR images.

Our findings also suggest that adding contrast-enhanced pulse sequences to the spinal cord assessment of patients already diagnosed with MS may be unnecessary. This aligns with the MAGNIS/NAIMS consensus [61]. This might help mitigate the potential long-term risks of gadolinium contrast agents.

## 6 References


1. Compston A, Coles A. Multiple sclerosis. Lancet. 2008 Oct 25;372(9648):1502-17. doi: 10.1016/S0140-6736(08)61620-7. PMID: 18970977.
2. Pearce, J. M. S. (2005). Historical Descriptions of Multiple Sclerosis. European Neurology, 54(1), 49–53.
3. Landtblom, AM., Fazio, P., Fredrikson, S. et al. The first case history of multiple sclerosis: Augustus d'Esté (1794–1848). Neurol Sci 31, 29–33 (2010).
4. Dobson, R. and Giovannoni, G., 2018. Multiple sclerosis – a review. European Journal of Neurology, 26(1), pp.27-40.
5. Kabat EA, Wolf A, Bezer AE. THE RAPID PRODUCTION OF ACUTE DISSEMINATED ENCEPHALOMYELITIS IN RHESUS MONKEYS BY INJECTION OF HETEROLOGOUS AND HOMOLOGOUS BRAIN TISSUE WITH ADJUVANTS. /J Exp Med/. 1947;85(1):117-130. doi:10.1084/jem.85.1.117
6. Jacobs LD, Cookfair DL, Rudick RA, et al. Intramuscular interferon beta-1a for disease progression in relapsing multiple sclerosis. The Multiple Sclerosis Collaborative Research Group (MSCRG) [published correction appears in Ann Neurol 1996 Sep;40(3):480]. /Ann Neurol/. 1996;39(3):285-294. doi:10.1002/ana.410390304
7. MS International Federation. Atlas of MS edition. Accessed September 6, 2023. https://www.msif.org/wp-content/uploads/2020/10/Atlas-3rd-Edition-Epidemiology-report-EN-updated-30-9-20.pdf.
8. Schwenkenbecher P, Wurster U, Konen FF, et al. Impact of the McDonald Criteria 2017 on Early Diagnosis of Relapsing-Remitting Multiple Sclerosis. Front Neurol. March 2019:10:188. doi:10.3389/fneur.2019.00188
9. Kingwell E, Leray E, Zhu F, Petkau J, Edan J, Oger J, Tremlett H, Multiple sclerosis: effect of beta interferon treatment on survival. Brain, Volume 142, Issue 5, May 2019:1324–1333, https://doi.org/10.1093/brain/awz055
10. Zahoor I, Haq E. Vitamin D and Multiple Sclerosis: An Update. In: Zagon IS, McLaughlin PJ, editors. Multiple Sclerosis: Perspectives in Treatment and Pathogenesis [Internet]. Brisbane (AU): Codon Publications; 2017 Nov 27. Chapter 5. Available from: https://www.ncbi.nlm.nih.gov/books/NBK470154/# doi: 10.15586/codon.multiplesclerosis.2017.ch5
11. Kjetil Bjornevik et al. Longitudinal analysis reveals high prevalence of Epstein-Barr virus associated with multiple sclerosis. Science. 375,296-301(2022). DOI:10.1126/science.abj8222

12. Simpson S Jr, Blizzard L, Otahal P, Van der Mei I, Taylor B. Latitude is significantly associated with the prevalence of multiple sclerosis: a meta-analysis. *J Neurol Neurosurg Psychiatry*. 2011;82(10):1132-1141. doi:10.1136/jnnp.2011.240432

13. Ghareghani M, Zibara K, Rivest S. Melatonin and vitamin D, two sides of the same coin, better to land on its edge to improve multiple sclerosis. *Proc Natl Acad Sci U S A*. 2023;120(14):e2219334120. doi:10.1073/pnas.2219334120

14. Hedström, A. K., Hillert, J., Olsson, T., & Alfredsson, L. (2013). Smoking and multiple sclerosis susceptibility. European journal of epidemiology, 28(11), 867-874.

15. Manouchehrinia, A., Tench, C. R., Maxted, J., Bibani, R. H., Britton, J., & Constantinescu, C. S. (2013). Tobacco smoking and disability progression in multiple sclerosis: United Kingdom cohort study. Brain, 136(7), 2298-2304.

16. Hedström, A. K., Ramanujam, R., Sundqvist, E., Hillert, J., Olsson, T., & Alfredsson, L. (2014). Smoking and two human leukocyte antigen genes interact to increase the risk for multiple sclerosis. Brain, 137(3), 835-843.

17. Brenner, P., Granqvist, M., Konigsson, J., Al Nimer, F., Piehl, F., & Jokinen, J. (2019). Depression and fatigue in multiple sclerosis: Relation to exposure to violence and cerebrospinal fluid immunomarkers. Psychoneuroendocrinology, 102, 185-190.

18. Harroud A, Mitchell RE, Richardson TG, et al. Childhood obesity and multiple sclerosis: A Mendelian randomization study. /Mult Scler/. 2021;27(14):2150-2158. doi:10.1177/13524585211001781

19. Ysrraelit MC, Correale J. Impact of sex hormones on immune function and multiple sclerosis development. Immunology. 2019;156(1):9-22. doi:10.1111/imm.13004

20. Valery N. Kornienko, I.N. Pronin. Diagnostic Neuroradiology. (2008) ISBN: 9783540756521 - Google Books

21. John Brust. CURRENT Diagnosis & Treatment in Neurology. (2006) ISBN: 9780071423663 - Google Books

22. Kurtzke JF. Rating neurologic impairment in multiple sclerosis: an expanded disability status scale (EDSS). Neurology. 1983;33(11):1444-1452.

23. Hobart, J., Lamping, D., Fitzpatrick, R., Riazi, A., & Thompson, A. (2001). The Multiple Sclerosis Impact Scale (MSIS-29): a new patient-based outcome measure. Brain, 124(5), 962-973.

24. Cohen, J.A., Reingold, S.C., Polman, C.H., & Wolinsky, J.S. (2012). Disability outcome measures in multiple sclerosis clinical trials: current status and future prospects. The Lancet Neurology, 11(5), 467-476.

25. Smith HJ. The history of magnetic resonance imaging and its reflections in Acta Radiologica. Acta Radiol. 2021;62(11):1481-1498. doi:10.1177/02841851211050857

26. Fechner, A., Savatovsky, J., El Methni, J., Sadik, J., Gout, O., Deschamps, R., Gueguen, A. and Lecler, A., 2019. A 3T Phase-Sensitive Inversion Recovery MRI Sequence Improves Detection of Cervical Spinal Cord Lesions and Shows Active Lesions in Patients with Multiple Sclerosis. American Journal of Neuroradiology, 40(2), pp.370-375.

27. Tench CR, Morgan PS, Jaspan T, Auer DP, Constantinescu CS. Spinal cord imaging in multiple sclerosis. /J Neuroimaging/. 2005;15(4 Suppl):94S-102S. doi:10.1177/1051228405283292

28. Loizou LA, Rolfe EB, Hewazy H. Cranial computed tomography in the diagnosis of multiple sclerosis. J Neurol Neurosurg Psychiatry. 1982;45(10):905-912. doi:10.1136/jnnp.45.10.905

29. Hemond CC, Bakshi R. Magnetic Resonance Imaging in Multiple Sclerosis. Cold Spring Harb Perspect Med. 2018;8(5):a028969. Published 2018 May 1. doi:10.1101/cshperspect.a028969

30. Thompson AJ, Banwell BL, Barkhof F, et al. Diagnosis of multiple sclerosis: 2017 revisions of the McDonald criteria. *Lancet Neurol*. 2018;17(2):162-173. doi:10.1016/S1474-4422(17)30470-2

31. National Multiple Sclerosis Society. Other conditions to rule out. Accessed September 6, 2023. https://www.nationalmssociety.org/Symptoms-Diagnosis/Other-Conditions-to-Rule-Out.

32. Wattjes, M., Steenwijk, M. & Stangel, M. MRI in the Diagnosis and Monitoring of Multiple Sclerosis: An Update. Clin Neuroradiol 25 (Suppl 2), 157–165 (2015).

33. Barkhof F, Filippi M, Miller DH, et al. Comparison of MRI criteria at first presentation to predict conversion to clinically definite multiple sclerosis. Brain. 1997;120 ( Pt 11):2059-2069. doi:10.1093/brain/120.11.2059

34. Nelson F, Poonawalla AH, Hou P, Huang F, Wolinsky JS, Narayana PA. Improved identification of intracortical lesions in multiple sclerosis with phase-sensitive inversion recovery in combination with fast double inversion recovery MR imaging. AJNR Am J Neuroradiol 2007;28:1645–1649.

35. Abidi Z, Faeghi F, Mardanshahi Z, Mortazavi H. Assessment of the diagnostic accuracy of double inversion recovery sequence compared with FLAIR and T2W_TSE in detection of cerebral multiple sclerosis lesions. Electron Physician. 2017 Apr 25;9(4):4162-4170. doi: 10.19082/4162. PMID: 28607651; PMCID: PMC5459288.

36. Wattjes MP, Lutterbey GG, Gieseke J, et al. Double inversion recovery brain imaging at 3T: diagnostic value in the detection of multiple sclerosis lesions. AJNR Am J Neuroradiol. 2007;28(1):54-59.

37. Favaretto A, Poggiali D, Lazzarotto A, Rolma G, Causin F, Gallo P. The Parallel Analysis of Phase Sensitive Inversion Recovery (PSIR) and Double Inversion Recovery (DIR) Images Significantly Improves the Detection of Cortical Lesions in Multiple Sclerosis (MS) since Clinical Onset. PLoS One. 2015;10(5):e0127805. Published 2015 May 26. doi:10.1371/journal.pone.0127805psir

38. Bruschi N, Boffa G, Inglese M. Ultra-high-field 7-T MRI in multiple sclerosis and other demyelinating diseases: from pathology to clinical practice. Eur Radiol Exp. 2020;4(1):59. Published 2020 Oct 22. doi:10.1186/s41747-020-00186-x

39. Mattay RR, Davtyan K, Bilello M, Mamourian AC. Do All Patients with Multiple Sclerosis Benefit from the Use of Contrast on Serial Follow-Up MR Imaging? A Retrospective Analysis. *AJNR Am J Neuroradiol*. 2018;39(11):2001-2006. doi:10.3174/ajnr.A5828

40. Bakshi, R., Thompson, A.J., Rocca, M.A., & Pelletier, D. (2008). MRI in multiple sclerosis: current status and future prospects. The Lancet Neurology, 7(7), 615-625.

41. Thornton, J.S., Ordidge, R.J., Penrice, J., Cady, E.B., Amess, P.N., Punwani, S., ... & Wyatt, J.S. (2010). Anisotropic water diffusion in white and gray matter of the neonatal piglet brain before and after transient hypoxia-ischaemia. Magnetic Resonance Imaging, 18(4), 397-403.

42. Guo BJ, Yang ZL, Zhang LJ. Gadolinium Deposition in Brain: Current Scientific Evidence and Future Perspectives. *Front Mol Neurosci*. 2018;11:335. Published 2018 Sep 20. doi:10.3389/fnmol.2018.00335

43. Gracia Bara MT, Gallardo-Higueras A, Moreno EM, et al. Hypersensitivity to Gadolinium-Based Contrast Media. *Front Allergy*. 2022;3:813927. Published 2022 Mar 17. doi:10.3389/falgy.2022.813927

44. Seta V, Gaouar H, Badaoui A, Francès C, Barbaud A, Soria A. Low-dose provocation and skin tests in patients with hypersensitivity to gadolinium-based contrast agents. *Clin Exp Allergy*. 2019;49(5):724-728. doi:10.1111/cea.13306

45. Tomás M, Fuentes Aparicio V, Zapatero Remon L, Alonso Lebrero E, Infante Herrero S. Skin reactions to gadolinium-based contrast media. *J Investig Allergol Clin Immunol*. 2012;22(4):292-293.

46. Wattjes MP, Ciccarelli O, Reich DS, et al. 2021 MAGNIMS-CMSC-NAIMS consensus recommendations on the use of MRI in patients with multiple sclerosis. /Lancet Neurol/. 2021;20(8):653-670. doi:10.1016/S1474-4422(21)00095-8

47. Koo TK, Li MY. A Guideline of Selecting and Reporting Intraclass Correlation Coefficients for Reliability Research [published correction appears in J Chiropr Med. 2017 Dec;16(4):346]. *J Chiropr Med*. 2016;15(2):155-163. doi:10.1016/j.jcm.2016.02.012

48. Akoglu H. User's guide to correlation coefficients. *Turk J Emerg Med*. 2018;18(3):91-93. Published 2018 Aug 7. doi:10.1016/j.tjem.2018.08.001

49. Lamb YN. Ocrelizumab: A Review in Multiple Sclerosis. /Drugs/. 2022;82(3):323-334. doi:10.1007/s40265-022-01672-9

50. Nij Bijvank JA, Sánchez Aliaga E, Balk LJ, Coric D, Davagnanam I, Tan HS, Uitdehaag BMJ, van Rijn LJ, Petzold A. A model for interrogating the clinico-radiological paradox in multiple sclerosis: Internuclear ophthalmoplegia. Eur J Neurol. 2021 May;28(5):1617-1626.

51. Stampanoni Bassi M, Gilio L, Buttari F, et al. Remodeling functional connectivity in multiple sclerosis: a challenging therapeutic approach. Front Neurosci. 2017; 11: 710.

52. Barkhof F. The clinico-radiological paradox in multiple sclerosis revisited. Curr Opin Neurol. 2002; 15(3): 239-245.

53. Mollison D, Sellar R, Bastin M, et al. The clinico-radiological paradox of cognitive function and MRI burden of white matter lesions in people with multiple sclerosis: a systematic review and meta-analysis. PLoS One. 2017; 12(5):e0177727.

54. Barkhof F, van Walderveen M. Characterization of tissue damage in multiple sclerosis by nuclear magnetic resonance. Philos Trans R Soc Lond B Biol Sci. 1999; 354(1390): 1675-1686.

55. Miller AE. An updated review of teriflunomide's use in multiple sclerosis. Neurodegener Dis Manag. 2021 Oct;11(5):387-409. doi: 10.2217/nmt-2021-0014. Epub 2021 Sep 16. PMID: 34486382.

56. Harel A, Ceccarelli A, Farrell C, Fabian M, Howard J, Riley C, Miller A, Lublin F, Inglese M. Phase-Sensitive Inversion-Recovery MRI Improves Longitudinal Cortical Lesion Detection in Progressive MS. PLoS One. 2016 Mar 22;11(3):e0152180. doi: 10.1371/journal.pone.0152180. PMID: 27002529; PMCID: PMC4803340.

57. Sethi V, Yousry TA, Muhlert N, Ron M, Golay X, Wheeler-Kingshott C, et al. Improved detection of cortical MS lesions with phase-sensitive inversion recovery MRI. J Neurol Neurosurg Psychiatry 2012;83:877–882. 10.1136/jnnp-2012-30302.

58. Cohen M, Bresch S, Thommel Rocchi O, Morain E, Benoit J, Levraut M, Fakir S, Landes C, Lebrun-Frénay C. Should we still only rely on EDSS to evaluate disability in multiple sclerosis patients? A study of inter and intra rater reliability. Mult Scler

Relat Disord. 2021 Sep;54:103144. doi: 10.1016/j.msard.2021.103144. Epub 2021 Jul 9. PMID: 34274736.

59. Shayganfar A, Sarrami AH, Fathi S, Shaygannejad V, Shamsian S. Phase sensitive reconstruction of T1-weighted inversion recovery in the evaluation of the cervical cord lesions in Multiple Sclerosis; is it similarly eligible in 1.5 T magnet fields? Mult Scler Relat Disord. 2018 Jul;23:17–22.

60. Karussis D. The diagnosis of multiple sclerosis and the various related demyelinating syndromes: a critical review. J Autoimmun 2014; 48–49: 134–142.

61. Knipe, H., Hacking, C. Spinal cord. Reference article, Radiopaedia.org. (accessed on 18 Apr 2022) https://doi.org/10.53347/rID-25075

62. Stroman PW, Wheeler-Kingshott C, Bacon M, Schwab JM, Bosma R, Brooks J, Cadotte D, Carlstedt T, Ciccarelli O, Cohen-Adad J, Curt A, Evangelou N, Fehlings MG, Filippi M, Kelley BJ, Kollias S, Mackay A, Porro CA, Smith S, Strittmatter SM, Summers P, Tracey I. The current state-of-the-art of spinal cord imaging: methods. Neuroimage. 2014 Jan 1;84:1070-81. doi: 10.1016/j.neuroimage.2013.04.124. Epub 2013 May 14. PMID: 23685159; PMCID: PMC4371133.

63. Nesbit GM, Forbes GS, Scheithauer BW, Okazaki H, Rodriguez M. Multiple sclerosis: histopathologic and MR and/or CT correlation in 37 cases at biopsy and three cases at autopsy. Radiology. 1991 Aug;180(2):467-74. doi: 10.1148/radiology.180.2.2068314. PMID: 2068314.

# Appendix

## Appendix 1: Approved Ethical Committee Application

**MEDIZINISCHE FAKULTÄT**
**DER CHRISTIAN-ALBRECHTS-UNIVERSITÄT ZU KIEL**

ETHIK-KOMMISSION

A.D. 1665

Ethik-Kommission · Schwanenweg 20 · 24105 Kiel

Dr. med. Sönke Peters
Dr. med. Friederike Gärtner
UKSH Kiel
Klinik für Radiologie und Neuroradiologie
Arnold-Heller- Straße 3, Haus D
24105 Kiel

Postadresse:
Arnold-Heller-Straße 3 / Haus U 27
D-24105 Kiel

Telefon 0431 / 500-14191
Telefax 0431 / 500-14195
ethikkomm@email.uni-kiel.de

Datum:
21. Dezember 2020

| | |
|---|---|
| **AZ Kiel:** | **D 624/20** (bitte stets angeben) |
| **Prüfplan:** | **Detektion von MS-Myelon-Läsionen mit einer 3D PSIR-Sequenz bei 1.5T (Retrospektive Auswertung)** Anschreiben v. 19.11.20; Basisformular v. 19.11.20; Studienprotokoll; Bewertungsbogen |
| **Studienleiter:** | **Dr. Sönke Peters, Dr. Friederike Gärtner, UKSH Kiel** |
| **Antrag vom:** | **19. November 2020 (Eingang: 24. November 2020)** |

Sehr geehrte Frau Kollegin Gärtner, sehr geehrter Herr Kollege Peters,

wir bestätigen den Eingang des obengenannten Antrages zur Beratung gemäß § 15 Berufsordnung (BO) der Ärztekammer Schleswig-Holstein. Nach Durchsicht der Unterlagen durch die Geschäftsstelle und durch mich als Vorsitzenden der Ethik-Kommission bestehen gegen die Durchführung der Studie keine berufsethischen und berufsrechtlichen Bedenken.

**Die im Folgenden aufgeführten Hinweise müssen beachtet werden:**
1.Es wird darauf hingewiesen, dass datenschutzrechtliche Aspekte grundsätzlich nur kursorisch durch die Ethik-Kommissionen geprüft werden. Dieses Votum ersetzt nicht die Konsultation des zuständigen Datenschutzbeauftragten.
2. Es wird darauf hingewiesen, dass künftige Änderungen der Studie der Ethik-Kommission anzuzeigen sind und gegebenenfalls eine erneute Beratung erforderlich machen.
3. Die ethische und rechtliche Verantwortung für die Durchführung dieser Studie verbleibt beim Studienleiter.
4. Die Ethik-Kommission weist darauf hin, dass für eventuell in Zukunft weitere teilnehmende Zentren eine berufsrechtliche Beratung bei der jeweils für sie zuständigen Ethik-Kommission erforderlich ist.
5. Gemäß Deklaration von Helsinki **muss** der Ethik-Kommission nach Studienende ein Abschlussbericht vorgelegt werden, der eine Zusammenfassung der Ergebnisse und Schlussfolgerungen der Studie enthält.
Wir wünschen Ihnen für die Durchführung der Studie viel Erfolg.

Mit freundlichen kollegialen Grüßen

Prof. Dr. med. H. M. Mehdorn
Vorsitzender der Ethik-Kommission

Dr. med. Christine Glinicke
Geschäftsführung der Ethik-Kommission

## Thanks & Acknowledgments

First and foremost, I extend my profound gratitude to Prof. Dr. med. Olav Jansen, Director of the Clinic for Radiology and Neuroradiology, for providing the conditions that made this study possible. I am sincerely thankful to PD Dr. habil. Dipl.-Phys. Mona Salehi Ravesh for her invaluable support, collaboration, and understanding throughout the course of this project. Her unwavering availability and guidance have been essential. Mona has been a true mentor in the research process. I am especially grateful for the time she dedicated to the initial project design and our joint work in imaging an amorphous agarose model.

I would also like to express my sincere gratitude to Dr. med. Sönke Peters. From the project's inception, Dr. med. Peters has worked with admirable motivation toward its completion. His commitment was integral in designing the project and supervising it until its successful acceptance for publication in late 2023. On top of that, I thank him for teaching me a considerable part of what I know about neuroradiology.

I also would like to thank the general support of my colleagues and friends at the Radiology and Neuroradiology Department of University Hospital Schleswig-Holstein, without which this journey would not have been as much fun as it was.

I thank all the patients who consented to participate in this study. Their contributions are invaluable, and I hope they will lead to a deeper understanding of this disease. I also wish to thank the radiology technicians for their collaboration and support throughout the MRI examinations.

I would also like to extend my heartfelt thanks to the team at the TORT Centre — Tayside Orthopaedic and Rehabilitation Technology Services — for their collaboration on my first scientific project in 2015-2016. A special mention goes to Dr. med. Rami J. Abboud, Dr. med. Graham Arnold, and Ian Christie. Cheers, mates!

I would like to thank my friends and family in Brazil for their patience and understanding regarding my life abroad. Many aspects of my life, including this project, would not have the same meaning without you.

## Publications

### Original article

#### 2024

Peters S, **Neves FB**, Huhndorf M, Gärtner F, Stürner K, Jansen O, Salehi Ravesh M. Detection of Spinal Cord Multiple Sclerosis Lesions Using a 3D-PSIR Sequence at 1.5 T. Clin Neuroradiol. 2024 Jan 30. doi: 10.1007/s00062-023-01376-x. Epub ahead of print. PMID: 38289376.

#### 2023

Gärtner F, Klintz T, Peters S, **Neves F**, Mostafa K, Mahnke J, Hensler J, Flueh C, Larsen N, Jansen O, Wodarg F. Intra-cranial aneurysm treatment with contour or WEB - a single center comparison of intervention times and learning curves. Interv Neuroradiol. 2023;10.1177/15910199231179512.

Mostafa K, **Neves F**, Gärtner F, Peters S, Hensler J, Larsen N, Klintz T, Mahnke J, Jansen O, Wodarg F. Contour device implantation versus coil embolization for treatment of narrow neck intracranial aneurysms. Sci Rep. 2023;13:10.1038/s41598-023-31877-1.

#### 2022

Mostafa K, Pfarr J, Langguth P, Schäfer JP, Trentmann J, Koktzoglou I, Edelman RR, Bueno **Neves F**, Graessner J, Both M, et al. Clinical Evaluation of Non-Contrast-Enhanced Radial Quiescent-Interval Slice-Selective (QISS) Magnetic Resonance Angiography in Comparison to Contrast-Enhanced Computed Tomography Angiography for the Evaluation of Endoleaks after Abdominal Endovascular Aneurysm Repair. /Journal of Clinical Medicine/. 2022; 11(21):6551.

#### 2018

**Neves FB**, Arnold GP, Nasir S, Wang W, MacDonald C, Christie I, Abboud RJ. Establishing state of motion through two-dimensional foot and shoe print analysis: A pilot study. Forensic Sci Int. 2018 Mar;284:176-183. doi: 10.1016/j.forsciint.2018.01.008. Epub 2018 Jan 31. PMID: 29408727.

**Letter to the editor**

**2022**

**Neves FB**, Jansen O, Trentmann J, Mostafa K, Madjidyar J. Minimally Invasive Treatment of a Cervical Aneurysmal Bone Cyst Through Percutaneous Doxycycline-Albumin Foam Injection. Cardiovascular and Interventional Radiology. 46. 1-3. 10.1007/s00270-022-03292-y.